13. SITE 1162[1]

Shipboard Scientific Party[2]

PRINCIPAL RESULTS

Site 1162 is located in Zone A ~90 km east of the ~127°E fracture zone and 40 km south of Site 1161. The seafloor magnetic age in this area is ~18 Ma. The site is located in a deep, wide, sediment-filled basin associated with an extinct westward-directed propagating rift. Site 1162 was selected as a complement to Site 1161 for two reasons: (1) it constrains the duration of the incursion of Indian-type mantle into Zone A that is recorded at Site 1161, and (2) it is located within the propagating rift valley, complementing the transferred lithosphere location of Site 1161. In both respects, the site is important to our understanding of the temporal and spatial limits of Indian-type mantle beneath the western part of Zone A.

Hole 1162A was spudded in 5464 m water depth and was washed through ~333 m of sediment, recovering a single wash barrel containing siliceous clay with a short interval containing tube casts and black chert clasts. Rotary drilling continued 31.4 m into volcanic basement, recovering 2.6 m (~8%) of mixed igneous clasts overlying a polymict fault breccia containing an array of clasts that can be divided into two metamorphic types. The first type is characterized by greenschist facies mineral assemblages (actinolite, chlorite, quartz, and epidote). Primary rock types include basalt, diabase, gabbro, and cataclasite. The second type is characterized by pervasive low-temperature alteration. A variety of basalts are more or less completely replaced by clay, and basaltic glass is extensively palagonitized. The distinctive mottled red and green breccia matrix is made up of finely divided, extensively altered igneous material and cemented by rhombohedral dolomite. Because it was unlikely to yield fresh volcanic samples suitable for analysis, Hole 1162A was abandoned.

Hole 1162B was spudded 200 m north of Hole 1162A and was washed through ~348 m of sediment, recovering 3.8 m of greenish gray

clay and an unconsolidated breccia with abundant altered basaltic clasts. Rotary drilling continued 58.9 m into basement, recovering 9.9 m (~17%) of dolomite (Unit 1) overlying dolomite-cemented basalt breccia (Unit 2). Basaltic clasts range from aphyric to highly plagioclase ± olivine phyric and are extensively altered, with groundmass replaced by clay throughout the hole.

A single glass sample from Hole 1162B was analyzed on board by inductively coupled plasma–atomic emission spectrometry (ICP-AES). As no fresh clean glass was recovered at this site, the analyzed sample contains 25%–30% spherulites. Its Ba content is at the high end and Zr/Ba is just outside the low end of the 0- to 7-Ma Pacific-type array. We interpret this as demonstrating a Pacific-type mantle affinity for this site. This confines the incursion of Indian-type mantle beneath Site 1161 to an ~80-km-wide region between Sites 1158 and 1162. Indian mantle was, therefore, present beneath this part of western Zone A for no more than 2–3 m.y., suggesting that the arrival of the propagating rift reintroduced Pacific-type mantle beneath the spreading axis.

OPERATIONS

Transit to Site 1162

The 27-nmi south-southeast transit from Site 1161 to Site 1162 required just over 3 hr at a speed of ~8 kt. Site 1162 is the second of three new sites surveyed on our transit between Sites 1158 and 1159 subsequently approved for drilling. Our seismic data indicated that a continuous sediment pond, >12 km across (north-south) and from 300 to >400 m deep, overlies strong reflectors interpreted to be volcanic basement. To optimize our drilling target, we conducted a 21-nmi, west-to-east single-channel seismic (SCS) survey across the Global Positioning System coordinates of our proposed site. A positioning beacon was dropped at 1525 hr 27 December where our seismic records indicated 200–300 m of sediment.

Hole 1162A

The precision depth recorder (PDR) depth referenced to the dual-elevator stool at Site 1162 is 5475.4 m. The nine-collar bottom-hole assembly (BHA) employed on the previous sites was reassembled with a new C-4 four-cone rotary bit made up to a mechanical bit release. We began Hole 1162A at 0015 on 28 December by washing down through 333.2 m of sediment and recovering a single wash barrel. Coring began when drilling conditions indicated a change from soft sediment to a harder formation. We advanced the hole by rotary coring from 333.2 to 364.6 meters below seafloor (mbsf) (Cores 187-1162A-2R to 5R; Table T1) with generally stable hole drilling conditions. After coring 31 m, we decided to abandon the hole because recovery was low (<10%) and the character of the recovered material indicated that we were coring down a fault zone. The predominantly cataclastic material is of little or no value in identifying the geochemical signature of the mantle source (our primary scientific objective), so the hole was terminated. As part of our continuing study on the infiltration of drilling fluid into the core, we deployed tracers of fluorescent microspheres on Cores 187-1162A-2R and 3R. The drill string cleared the seafloor at 0100 hr on 29 December, and we offset in dynamic positioning mode 200 m north.

T1. Coring summary, Site 1162, p. 44.

Hole 1162B

We began drilling Hole 1162B with a wash barrel in place at 0215 hr on 29 December. After washing through 348.4 m of sediment and encountering a change in drilling conditions, we recovered the wash barrel and began rotary coring. Hole 1162B was advanced from 348.4 to 407.30 mbsf (Cores 187-1162B-2R to 11R) at an average penetration rate of 3 m/hr. We terminated coring when the time allocated to this site during our active planning process expired, even though we had not recovered material we could interpret as basaltic basement. Nevertheless, we expect to be able to use a few basalt fragments recovered from this site with shore-based analytical tools to reach our objectives. We deployed microsphere tracers on Cores 187-1162B-2R and 11R. The average recovery for Site 1162 was 14%.

The drill bit cleared the seafloor at 0245 hr on 31 December. During this pipe trip, the rig crew conducted the end-of-the-leg nondestructive examination of the BHA. The bit cleared the rotary table at 1345 hr on 31 December, concluding operations at this site.

IGNEOUS PETROLOGY

Introduction

Holes 1162A and 1162B were cored into igneous basement at this site. Hole 1162A penetrated 31.4 m into basement, recovering 2.58 m of rock in four cores (Cores 187-1162A-2R to 5R), a net recovery of 8.22%. Hole 1162B penetrated 58.9 m into basement, recovering 9.94 m of rock in 11 cores (Cores 187-1162B-1W to 11R), a net recovery of 16.88%. The dominant lithology in these two holes is a dolomite-cemented basalt breccia that contains a variety of highly altered basaltic clasts, some of which have undergone greenschist facies metamorphism.

Hole 1162A

The recovered material from this hole has been assigned to two lithologic units: mixed igneous clasts (Unit 1) and a dolomite-cemented basalt breccia (Unit 2).

Unit 1

This unit consists of the two pieces in Section 187-1162A-2R-1. Piece 1 is a greenschist facies metabasalt. It is part of a complex glassy chilled margin which has red-purple and brown-red subvertical planar bands of coalesced spherulites (Fig. F1) in a dark olive-green matrix. The spherulites increase in size (from <0.4 to ~2 mm) with distance from the outer edge of the piece.

A single, ~4-mm-long plagioclase xenocryst can be seen in thin section (Fig. F2). It has an oval outline, suggesting that it is out of equilibrium with its host, and it contains two large (~0.1–0.6 mm) irregularly shaped melt inclusions. Rare altered olivine microlites (up to 0.2 mm) are also present in areas of coalesced spherulites. The spherulites have been partially to totally replaced by a mixture of chlorite and actinolite, as has much of the groundmass. Epidote (~2%) is present as discrete, irregularly shaped, equant grains (<0.2 mm) in cloudy regions of the

F1. Spherulite pseudomorphs in the chilled margin of a metabasalt, p. 16.

2 mm
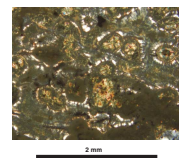
F2. Plagioclase xenocryst in metabasalt, p. 17.

4 mm
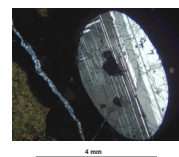
groundmass. Minor amounts of chlorite occur in association with quartz replacing mesostasis between spherulites in part of the sample. Based on the presence of crystal pseudomorphs (as long as 0.4 mm) having swallowtail prism shapes, we conclude plagioclase was originally present in the groundmass (~10%), where it usually occurs in the centers of spherulites. Whisker-like quench growth crystals nucleated around the perimeter of the xenocryst discussed above (Fig. F3), testifying to a rapid cooling rate for the protolith. Quartz with undulose extinction is present in veins.

Piece 2 is a brown to orange-brown, very highly altered, moderately plagioclase phyric basalt. Rounded to prismatic plagioclase is the sole phenocryst phase, constituting ~2% of the rock. The groundmass is fine grained and is replaced by brown clay and locally by Fe oxyhydroxide.

Unit 2

Twenty-eight of the 48 pieces in Cores 187-1162A-3R to 5R are dolomite-cemented basalt breccia. The remaining 20 pieces are single clasts, some with adhering matrix. Consequently, all three of the remaining cores from Hole 1162A (Cores 187-1162A-3R to 5R) are included in one lithologic unit: a dolomite-cemented basalt breccia. The three types of clast are basalt (14 pieces), metagabbro and metadiabase (five pieces), and cataclasite (one piece). The polymict breccia is generally red or green and poorly sorted. The clast:matrix ratio is ~80:20 throughout this hole. Unlike breccias from earlier sites, there is little or no Mn oxide coating on the clasts in this breccia, and Mn oxide is rare in the matrix.

Subangular to subrounded clasts of aphyric to highly phyric basalt, cataclasite, metagabbro, metadiabase, and palagonite range in size from <0.5 mm to >3 cm. The relative proportions of the clast types vary throughout the core. For example, Section 187-1162A-4R-1 is dominated by basaltic clasts, whereas Section 187-1162A-5R-2 is dominated by basalt clasts with minor metagabbro and metadiabase clasts. Palagonite is rare, usually present as highly altered (see "Alteration," p. 7) small (<1 mm) grains. Crystalline epidote clasts (see "Alteration," p. 7) are small (<1.5 mm) and rare (<3%) (e.g., Section 187-1162A-4R-1 [Piece 3]). Clast size also varies within the recovered section. For example, in Section 187-1162A-3R-1, clasts are bimodal, ranging from <0.5 to 10 mm and 20 to >30 mm, whereas clasts in Section 187-1162A-4R-1 range from <0.5 to 80 mm. All clasts are moderately to very highly altered and are commonly fractured in situ into three or more pieces; the fractures are infilled with matrix, separating the subpieces by ~2 mm (e.g., Section 187-1162A-3R-1 [Piece 1]). There are no alteration halos around clasts, and clasts with different degrees of alteration from different metamorphic facies are intermixed.

Petrography of Clasts

Aphyric to Highly Phyric Basalt

The color of these clasts ranges from brownish gray in the fresher pieces (moderately altered) to brown in the very highly altered pieces. Pieces 5–8 in Section 187-1162A-5R-2 are highly plagioclase-olivine phyric basalt, Pieces 8–14 and 16 from Section 187-1162A-5R-1 are aphyric to moderately plagioclase-olivine phyric basalt, and Pieces 1–5 in Section 187-1162A-3R-1 are sparsely plagioclase phyric basalt.

F3. Quench overgrowths on the edge of an oval plagioclase xenocryst, p. 18.

0.5 mm

Olivine phenocrysts vary in abundance from 0% to 4% and are totally altered (e.g., Section 187-1162A-5R-1 [Piece 15]; see "Alteration," p. 7) but appear to have been equant, ranging from 0.5 to 1.5 mm in size.

Plagioclase has a larger range in both abundance and size (0%–20% and 0.5–8 mm). Plagioclase phenocrysts commonly display disequilibrium textures (such as concentric oscillatory zoning and corroded cores) that are partially replaced by clay mixtures (e.g., Section 187-1162A-5R-1 [Piece 15]). In Section 187-1162A-5R-1 (Piece 16), clusters of large (~2 mm) plagioclase phenocrysts have undulose (strain) extinction and have formed new subgrain boundaries across which the original oscillatory zoning continues (Fig. F4).

The groundmass is fine grained (generally <1 mm) and originally contained plagioclase and clinopyroxene in nearly equal proportions along with ~3% opaque minerals; the texture is subophitic. Approximately 25% of the clinopyroxene is variably replaced by clay, prismatic actinolite as long as 1 mm, and some chlorite.

Metagabbro and Metadiabase

Piece 14 from Section 187-1162A-4R-1 and Pieces 1, 2, 5, 6, and 7 from Section 5R-1 are metagabbro and metadiabase, distinguished from the basalts by their larger grain size and more granular textures (~4 mm in Section 187-1162A-4R-1 [Piece 14] vs. ~1.5 mm in Section 5R-1 [Piece 6]). The color is speckled dark green and cream, reflecting the greenschist facies assemblage of amphibole and plagioclase. The original igneous mineralogy of this clast type was ~49% plagioclase, ~45% clinopyroxene, 5% opaque minerals (mainly ilmenite), and 1% olivine.

As much as 3% of the plagioclase crystals in some pieces of the metadiabase (e.g., Section 187-1162A-5R-1 [Piece 7]) are coarse grained (~3 mm), relative to the medium-grained matrix plagioclase (~1 mm). The large crystals are subhedral laths that have disequilibrium textures, such as disrupted twinning, oscillatory zoning, and corroded cores. There is some replacement by clay along fractures. The remaining plagioclase (~46%) in the matrix is subhedral and tabular to prismatic; some crystals show zoning, radial growth, or undulose extinction. In one metagabbro piece (Section 187-1162A-4R-1 [Piece 14]), plagioclase varies from ~1 to 8 mm in size.

Olivine was present only as relatively large crystals (~3 mm) and has been totally replaced by complex concentric halos of talc and opaque minerals around prismatic cummingtonite? (Fig. F5).

In the metadiabase, clinopyroxene has an average size of ~1.2 mm and partially encloses matrix plagioclase (~1 mm). However, ~85% of the clinopyroxene has been replaced by actinolite and some chlorite (Fig. F6A, F6B).

Cataclasite

The cataclasite clast (Section 187-1162A-4R-1 [Piece 13]) is dark green and consists of parallel sets of 1–3 mm wide gray-green shear bands that are oriented at ~30° to the core axis and connected by subvertical ~0.5-mm-wide shear bands to form a conjugate set (see "Structural Geology," p. 12). The clasts in the cataclasite are highly altered aphyric basalt ranging from 1 mm to 4 cm in size. The matrix is green-gray, silt-sized mylonite that is possibly altered to actinolite/chlorite.

F4. A plagioclase glomerocryst in altered metabasalt, p. 19.
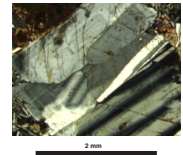
F5. Altered olivine phenocryst in metadiabase, p. 20.
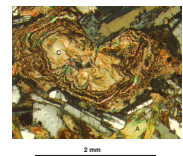
F6. Altered clinopyroxene in metagabbro, p. 21.
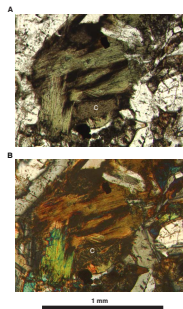
Matrix

The matrix consists of ~75% granular to crystalline rhombohedral dolomite (does not react with dilute HCl [~5%–10%] until crushed and heated) and clay- to silt-sized lithic particles of igneous material. Two main matrix colors (red and green) are observed, and these occur together in individual pieces as bands (e.g., throughout Pieces 1A, 1B, and 1C in Section 187-1162A-5R-2). We assume the green color is due to the presence of chlorite and the red color to the presence of Fe-stained clays. In Pieces 1A, 1B, and 1C in Section 187-1162A-5R-2, the largest clasts in the red matrix (1.5–2.0 cm) are smaller than those in the green matrix (2.5–3.5 cm). The clasts in the red matrix are mainly highly altered, brown, fine-grained, aphyric to plagioclase phyric basalt, whereas clasts in the green matrix are metagabbro and metadiabase. In Section 187-1162A-5R-1 (Piece 18), the chloritized green matrix has a linear fabric that is aligned in oblique shear bands ~5 mm wide which appear to partially wrap around clasts.

Irregular cavities (as wide as 10 mm) are lined by distorted, colorless rhombohedra (~0.8 mm) of dolomite, commonly forming saddle-shaped crystals (e.g., Section 187-1162A-5R-2 [Piece 4]).

Hole 1162B

The recovered material from this hole has been assigned to two lithologic units: dolomite and dolomite-cemented basalt breccia.

Unit 1

This unit consists of Pieces 1–3 from Section 187-1162B-1W-3, which are pink-brown to mottled pink and cream, fine-grained dolomite. The three pieces are increasingly lithified downhole. Piece 1 consists of a gray-pink mottled soft sediment mostly composed of crystals of dolomite <0.2 mm across. The irregular gray blotches are scattered Mn oxide grains associated with Mn oxide–stained halos up to 1.5 cm wide. Piece 3 is coarser grained (~0.2 mm) than Piece 1 and has clasts of highly altered, concentrically banded, yellow palagonite (<1 mm) in areas of coarser grained (~0.3 mm) dolomitic sediment. These coarser grained areas have borders of Mn oxide dendrites that project into the finer-grained sediment.

Unit 2

This unit is a poorly sorted dolomite-cemented basalt breccia, similar to Unit 2 in Hole 1162A. However, there are some differences between the two holes. In Hole 1162B, the clast:matrix ratio varies from 20:80 (e.g., Section 187-1162B-3R-2) to 80:20 (e.g., Section 11R-1) but averages ~50:50. The matrix is lighter in color, being white to buff rather than red and green.

Clasts

In contrast to Unit 2 of Hole 1162A, all of the breccia clasts in Hole 1162B are basaltic. They are subangular to subrounded and aphyric to highly phyric, and in this sense are similar to the basalt clasts in Hole 1162A. They are, however, more highly altered, the groundmass having been ~95% replaced by clays throughout this hole. Consequently they are brown. Up to 50% of the phenocrysts occur in glomerocrysts (as long as 6 mm) of olivine and plagioclase that consist of numerous (>10)

small (<0.5 mm) euhedral crystals (e.g., Section 187-1162B-1W-3 [Pieces 4–7]). Some basalt clasts have chilled margins (e.g., Section 187-1162B-3R-1 [Piece 22]; Fig. F7). Palagonite is also present as a clast and ranges from orange brown near the top of the unit to yellowish green and green toward the bottom, the latter color being an indication that the palagonite has been replaced by clay (see "Alteration," p. 7). The palagonite tends to be concentrically zoned (Fig. F8).

In general, basalt clasts are larger (3–70 mm) than the palagonite clasts (<1–17 mm). They also commonly show signs of in situ disaggregation similar to that seen in Hole 1162A (e.g., Section 187-1162B-3R-1 [Piece 22]; Fig. F8). Possible slickensides were identified by the presence of cryptocrystalline silica on the side of a basalt clast in Section 187-1162B-3R-1 (Piece 21). Approximately 30% of all clasts have Mn oxide coatings, which contrast with the breccia in Hole 1162A.

Matrix

The matrix is white to buff in color and is made up of granular dolomite + clay to silt-sized particles of dolomite and detrital igneous material. Thin (~1 mm) halos of intergrown rhombohedral dolomite outline many of the clasts in the breccia (e.g., Section 187-1162B-3R-1 [Piece 22]; Fig. F7). In addition, the matrix surrounding some basalt clasts below Section 187-1162B-7R-1 (e.g., Piece 1) is stained red, particularly where the red-brown highly altered basalt clasts have complex reaction rims. These zones in the matrix are 1–2 mm wide, with colorless crystalline dolomite next to the clast, followed by a red-stained halo in the matrix. This is observed even for small clasts (~1–2 mm). This process of Fe staining also affects the green palagonite clasts, partially altering them to an orange color. Mn oxide nodules (~0.5–2 mm in diameter) are common. The matrix is dissected by a meshwork of numerous colorless crystalline dolomite veins 0.2–2 mm wide. In Section 187-1162B-3R-1, intense net-veining by clear crystalline dolomite has isolated angular remnants of pink dolomite matrix. In places the matrix reacts more readily with dilute HCl than does the Hole 1162A matrix. This may indicate the matrix contains a significant amount of calcite, although chemical analysis of two samples (Section 187-1162B-5R-1 [Pieces 3 and 24]) by ICP-AES indicates a Ca:Mg ratio appropriate for dolomite; an X-ray diffraction scan of the same samples also displayed dominant dolomite peaks (see "Geochemistry," p. 14).

ALTERATION

Hole 1162A

In Hole 1162A moderately to highly altered basalt occurs as single fragments in Units 1 and 2 and as basalt clasts within a dolomite-cemented breccia in Unit 2 (see "Igneous Petrology," p. 3). Since basalt fragments from Unit 1 have alteration characteristics similar to those of Unit 2, the two are discussed together. Alteration conditions in Hole 1162A range from low-temperature to lower greenschist facies.

Greenschist Facies Alteration

Greenschist facies alteration has affected most types of breccia clasts, including both aphyric and sparsely to moderately plagioclase olivine phyric basalt (Sections 187-1162A-3R-1, 5R-1, and 5R-2), microgabbro

F7. Dolomite-cemented basalt breccia, p. 22.
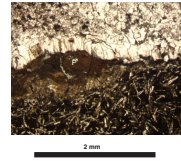
F8. Palagonite clast with concentric zoning, p. 23.

(Sections 187-1162A-4R-1 and-5R-1), dark green metabasalt (Section 187-1162A-2R-1 [Piece 1]), dark green basaltic cataclasite (Section 187-1162A-4R-1 [Piece 13]), and moderately plagioclase phyric basalt (Section 187-1162A-2R-1 [Piece 2]). Veins are rare, but, where present, they are 0.5–2 mm wide and filled with chlorite, white cryptocrystalline silica (Section 187-1162A-2R-1 [Piece 1]), or colorless crystalline dolomite (Sections 5R-1 and 2), the latter being similar to the matrix of the breccia.

In hand specimen, the aphyric and plagioclase olivine phyric basalts are greenish brown and appear highly altered (40%–60%) throughout (Fig. F9). When viewed with a hand lens, groundmass olivine and clinopyroxene appear to be extensively replaced by Fe oxyhydroxide and clay in most pieces, except for Section 187-1162A-3R-1 (Piece 4), which has a chloritized groundmass. About 40% of the plagioclase phenocrysts in that piece are opaque and cream colored. In some places, plagioclase is discolored (darkened) by Mn oxide linings along crystal faces and microcracks (e.g., Sections 187-1162A-5R-1 and 5R-2); elsewhere it is mostly transparent and relatively fresh. Olivine phenocrysts are totally replaced by Fe oxyhydroxide and/or a pale yellowish mineral, identified in thin section as a mixture of mostly chlorite, talc, clay, and Fe oxyhydroxide (Figs. F10, F11). Plagioclase phenocrysts commonly are clay lined along crosscutting fractures but are otherwise fresh. In thin section, groundmass olivine and clinopyroxene are mostly replaced by chlorite (Fig. F12) and clay. The presence of chlorite indicates that these rocks underwent low-temperature metamorphism at 150°–250°C (Alt et al., 1996), which left the overall textural relationships of the rock intact. Such alteration conditions have not been observed at our earlier sites. The presence of Fe oxyhydroxide in the centers of some olivines that are rimmed by chlorite and talc indicates metamorphic disequilibrium.

Similar observations are made for the dark green to cream, vein-free metadiabase (Fig. F13). In hand specimen the rock appears highly altered, and, except for plagioclase, mineral phases are difficult to identify. In thin section, fibrous actinolite and chlorite mostly replace (20%–38%) the original (45%) clinopyroxene (Fig. F14). Olivine is totally replaced by concentric layers of talc, chlorite, and magnetite with cummingtonite? in the center (Fig. F15). Plagioclase is partially replaced (~20%) by clay + chlorite and recrystallized to albite along crystal margins. Numerous microveins (<25/m) are filled with chlorite and clay. The presence of actinolite + talc + chlorite + albite is consistent with metamorphism in the lower greenschist facies (Alt et al., 1996).

The dark green metabasalt fragment in Section 187-1162A-2R-1 (Piece 1) contains a wide, complex spherulitic quench zone in which the spherulites are partially to completely replaced by actinolite. Actinolite, chlorite, and epidote pervasively replace the groundmass (Fig. F16). Recrystallized quartz veins dissect the groundmass and show strain extinction and preferred orientation of crystallographic axes, indicating temperatures of at least 150°C. Again, the presence of the secondary mineral assemblage actinolite + chlorite + quartz ± epidote indicates lower greenschist facies metamorphism (Alt et al., 1996).

Cataclasites

The 10 cm × 5 cm piece of basaltic cataclasite (Fig. F17) is dominated by 1- to 3-mm-wide parallel sets of greenish gray shear zones (see "Structural Geology" p. 12) oriented 40°–30° from vertical and linked

F9. Highly altered, moderately plagioclase-olivine phyric basalt, p. 24.
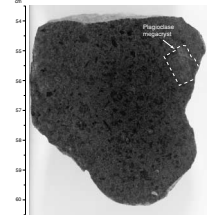
F10. Altered olivine phenocryst, p. 25.
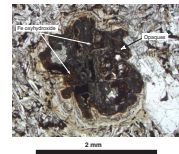
F11. Olivine microphenocryst replaced by chlorite, talc, and opaques, p. 26.
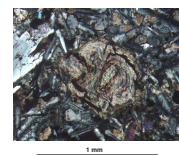
F12. Replacement of groundmass clinopyroxene by chlorite, p. 27.
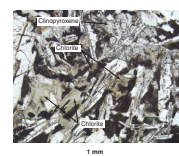
F13. Highly altered metadiabase, p. 28.
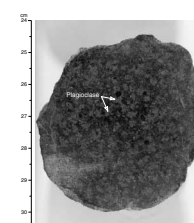
by a network of smaller (<0.5 mm) subvertical shear relay zones. The two sets of shear planes divide the rock into angular domains of undeformed, light, altered aphyric basalt that appear to indicate brittle deformation. These domains are cut by minute veins that are filled with the same material as the larger shear zones. This greenish gray silt-sized matrix probably consists of chlorite and intensely ground basalt clasts.

Chlorite Layers Crosscutting Dolomite

In Section 187-1162A-5R-1 (Pieces 18 and 20), green chlorite is present as several millimeter-wide layers within the crystalline dolomite matrix. In Piece 18, the chlorite-rich zones appear to reflect small-scale shear zones. The presence of chlorite in these breccia pieces indicates elevated temperatures in the range of 150°–250°C, again suggesting metamorphic disequilibrium.

Low-Temperature Alteration

A brown to orange-brown, very highly altered, moderately plagioclase phyric basalt in Section 187-1162A-2R-1 (Piece 2) is exceptional in alteration mineralization. It is the only basalt fragment in this hole in which the groundmass is mostly replaced by brown clay and Fe oxyhydroxide, indicating low-temperature alteration conditions; this is a distinct contrast to the predominant lower greenschist facies alteration of the other basalt fragments. It may be an intensely weathered greenschist facies basalt.

The poorly sorted, dolomite-cemented breccia has clast:matrix ratios ranging from 80:20 to 90:10. The majority of angular to subangular clasts range from 30 to <1 mm, but occasionally they measure up to 80 mm × 35 mm (Section 187-1162A-4R-1 [Piece 4]). The clasts are predominantly aphyric basalt. Notably, and unlike previous sites, Mn oxide is almost absent from the surfaces of clasts and is rare in the dolomite matrix. Small (<1–4 mm) palagonite clasts are restricted to Section 187-1162A-3R-1. Clasts of epidote are present only in Section 187-1162-4R-1 (Piece 3). Clasts consisting of basaltic cataclasite and plagioclase-olivine phyric basalt, similar to the single pieces described above, are present in Sections 187-1162A-4R-1 (Pieces 4 and 5) and 5R-1 (Piece 17), respectively. A few clasts that appear to be fractured in situ (e.g., Section 187-1162A-3R-1 [Piece 1]) are cut by veins (as wide as 2 mm) that are filled with crystalline dolomite similar to that of the breccia matrix. The aphyric basalt clasts are highly altered, except for a few moderately altered clasts in Section 187-1162A-4R-1 (Pieces 1–6).

No alteration halos are associated with the veins or with the clast margins. This indicates that alteration was pervasive and took place prior to formation of the breccia. Olivine and clinopyroxene in the groundmass of the aphyric basalt clasts are mostly replaced by clay and Fe oxyhydroxide, consistent with low-temperature alteration. The matrix of the basalt breccia consists of crystalline dolomite (Fe stained in places), the mineralogy and chemistry of which are treated in more detail in "Igneous Petrology," p. 3.

In conclusion, two alteration or metamorphic facies, (1) low temperature and (2) lower greenschist, are recognized in Hole 1162A and do not vary systematically downhole. Because greenschist facies alteration is restricted to individual pieces and a few smaller breccia clasts, whereas low-temperature alteration is pervasive in most breccia clasts, the greenschist facies rocks must have been derived from a source out-

side the location of Hole 1162A. The secondary mineral assemblage act-inolite + chlorite + talc + albite reflects hydrothermal alteration at 250°–350°C (Alt et al., 1996). The setting of Hole 1162A at the margin of a deep (~5500 m), fault-bounded basin next to a comparatively shallow (~4000–3500 m) ridge, together with the presence of cataclasite frag-ments in the core, suggest that exhumed, lower greenschist facies rocks of the deeper volcanic section were exposed and eroded along the flanks of the ridge. Both greenschist facies and low-temperature altered basaltic clasts formed a breccia that was subsequently cemented by do-lomite and then deformed again. The low-temperature rocks would be derived from a shallower part of the volcanic section, either locally or from the upper parts of the ridge.
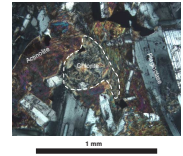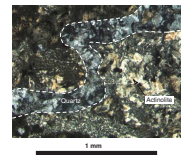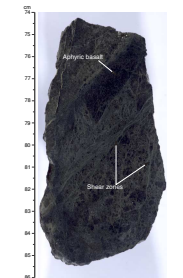
Hole 1162B

Unit 1 of Hole 1162B is exclusively pale pinkish dolomite (see **"Igne-ous Petrology,"** p. 3). Unit 2 consists of highly to very highly altered, angular to subangular, basalt clasts in a dolomite-cemented breccia. Be-cause numerous basalt pieces have matrix breccia attached to their mar-gins, basalt and breccia pieces are considered as a single lithologic Unit 2.

Basaltic clasts range from 30 to 70 mm and include both aphyric and slightly to moderately plagioclase-olivine phyric basalts, all of which are highly (40%–80%) to very highly (80%–95%) altered (Fig. **F18**). Mi-nor fractures and veins are either narrow and Mn oxide lined or as wide as a millimeter and filled with crystalline dolomite, similar to that of the breccia matrix. Alteration halos are rare (e.g., Section 187-1162B-4R-1 [Piece 1]), but the vast majority of basalt fragments show pervasive, low-temperature groundmass alteration of olivine, clinopyroxene, and, in places, plagioclase, to brown clay and Fe oxyhydroxide. Olivine phe-nocrysts are 100% replaced by Fe oxyhydroxide and clay. In very highly altered sections (such as Section 187-1162B-5R-1), plagioclase pheno-crysts are 20%–50% replaced by clay and Fe oxyhydroxide. In less al-tered sections, plagioclase phenocrysts are relatively fresh. Chilled margins are minor and distributed throughout the hole; within these, fresh glass is rare (e.g., Section 187-1162B-5R-1 [Pieces 17 and 19]). Most of the glass has been replaced by layered palagonite up to a milli-meter thick (Fig. **F18**).

The dolomite-cemented basalt breccia is poorly sorted with a clast:matrix ratio that increases downhole from ~40:60 in Sections 187-1162B-1W-3 through 7R-1 to ~80:20 in Sections 7R-1 through 11R-1, except for Sections 3R-2 and 6R-1 (20:80 and 10:90, respectively). The two principal clast types are <5- to 50-mm aphyric and slightly to mod-erately plagioclase-olivine phyric basalt and 1- to 15-mm palagonite. In contrast to Hole 1162A, ~30% of the basalt clasts have surface patches of Mn oxide from a few millimeters to a centimeter across. In numerous places, the basalt clasts are dissected by 0.5- to 3-mm-wide veins that are connected with the breccia matrix and filled by crystalline dolo-mite, similar to that of the breccia matrix (Fig. **F19**). These relationships suggest in situ fracturing during or after breccia formation. No alter-ation halos are associated with these veins, suggesting that the perva-sive clast alteration predates veining. Throughout the hole, the basalt clasts are highly (40%–80%), often very highly (80%–95%) or even completely, altered. Alteration is manifested by thorough replacement of groundmass olivine, clinopyroxene, mesostasis, and, in places, pla-gioclase by clay and Fe oxyhydroxide (Fig. **F20**). Red-brown coloration,

F18. Highly altered sparsely pla-gioclase-olivine phyric basalt, p. 33.

F19. Dolomite-cemented basalt breccia, p. 34.
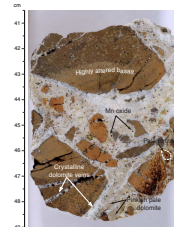
F20. Groundmass clinopyroxene and plagioclase replaced by smec-tite and Fe oxyhydroxide, p. 35.
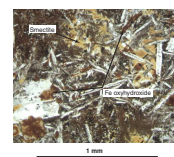
softening by clay, and large open fractures that formed after the core was split (as a result of contraction during drying) reflect the high clay abundance in these altered basalt clasts (Fig. F21). Olivine phenocrysts are totally replaced by Fe oxyhydroxide and clay. Plagioclase phenocrysts are also mostly replaced by clay and Fe oxyhydroxide.

Palagonite clasts are less abundant (10%–20%) and smaller (mostly 1–15 mm) than the basalt clasts. In the 1- to 3-mm range, palagonite dominates over basalt in some sections (e.g., Section 187-1162B-5R-1). Palagonite ranges in color from orange or reddish brown to yellowish green to pale yellow beige. Concentric layering is common; the centers of clasts tend to be reddish and the outer margins yellowish green. The yellowish green palagonite is softer than the reddish brown palagonite, suggesting a higher abundance of clay, which can be interpreted to reflect alteration of palagonite itself (Fig. F8).

The breccia matrix is described in detail in "Igneous Petrology," p. 3. It consists of two generations of dolomite. The first is clay rich and intensely brecciated and veined by second-generation crystalline dolomite (Fig. F22). Mn oxide spots (0.5–2 mm) appear to be exclusively associated with the first-generation clay-rich dolomite (Fig. F19).

In conclusion, low-temperature alteration is pervasive in Hole 1162B; the most intensely altered basalts recovered during Leg 187 are from this site.

MICROBIOLOGY

Four rock samples (Samples 187-1162A-3R-1 [Piece 3, 10–14 cm], 187-1162A-5R-1 [Piece 19, 99–102 cm], 187-1162B-2R-1 [Piece 1, 1–5 cm], and 187-1162B-6R-1 [Piece 25, 133–136 cm]) were collected at Site 1162 to characterize the microbial community inhabiting this environment (Table T2). All samples were breccia fragments. To sterilize them, the outer surfaces of the rocks were quickly flamed with an acetylene torch, and enrichment cultures and samples for DNA analysis and electron microscope studies were prepared (see "Igneous Rocks," p. 7, in "Microbiology" in the "Explanatory Notes" chapter).

Fluorescent microsphere tests were carried out for four rock cores to evaluate the extent of contamination caused by drilling fluid (see "Tracer Test," p. 9, in "Microbiology" in the "Explanatory Notes" chapter and Table T2). Pieces of rock from each core were rinsed in nanopure water, and the collected water was filtered. Thin sections were used to examine the extent of contamination inside some samples. Filters and thin sections were examined under a fluorescence microscope for the presence of microspheres. Microspheres were detected on all four filters; in the thin sections, microspheres were located both inside fractures and on thin-section surfaces. The microspheres on the polished surfaces were most often found close to fractures or to thin-section (i.e., piece) margins and may have been relocated by polishing. Thirty-seven microspheres were observed in thin sections from Core 187-1162A-2R, two from Core 187-1162B-2R, and 45 from Core 187-1162B-11R. Core 187-1162B-11R had a very low recovery; therefore, no thin sections were made.

F21. Dolomite-cemented basalt breccia with highly altered basalt fragments displaying shrinkage cracks, p. 36.
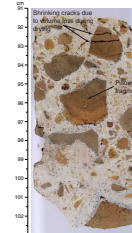
F22. Crystalline dolomite vein cutting an altered basalt clast, p. 37.

T2. Rock samples for cultures, DNA analysis, SEM/TEM, and contamination studies, p. 45.

STRUCTURAL GEOLOGY

Recovered material from Site 1162 is predominantly breccia. In Hole 1162A, clasts, which make up ~90% of the breccia, include aphyric to highly phyric basalt, palagonite, cataclasite, and metadiabase (see **"Igneous Petrology,"** p. 3). The cataclasite clast recovered in Section 187-1162A-4R-1 (Piece 13, 74–87 cm) (Fig. **F23**) contains an ultracataclasite (Ramsay and Huber, 1987) zone ~1 cm wide and several narrow shear zones. No structures indicating the sense of shear or the mode of deformation were observed.

Fractures and veins are scattered throughout the clasts from Hole 1162A. The fracture + vein density ranges from 0 to 30.0/m and averages 4.2/m. The vein density ranges from 0 to 30.0/m and averages 3.2/m.

The breccia in Hole 1162B resembles that previously recovered from Site 1156. Clasts include aphyric to highly phyric basalts with a matrix of micritic carbonate cut by crystalline carbonate veins.

Fractures and veins are less common than in Hole 1162A. Fifteen fractures and only one vein occur between Cores 187-1162A-2R and 11R. The fracture + vein density ranges from 0 to 6.5/m and averages 1.2/m. The vein density averages 0.1/m. The breccia may have a lower density of fractures and veins because the clasts broke along preexisting fractures and veins during brecciation.

SITE GEOPHYSICS

Site location for Site 1162 was based on a Leg 187 SCS survey conducted during transit from Site 1158 to Site 1159 (*JOIDES Resolution* [JR] survey line S7; Fig. **F24**). The roughly north-south seismic profile between shots 1074 and 1283 shows a ~12-km-wide basin structure with sediment cover >300 m. (see site AAD-39a in Fig. **F16,** p. 22, in the "Site 1159" chapter [AAD = Australian Antarctic Discordance]). The prospectus site AAD-39a is near shotpoint 2425, located slightly toward the northern side of the basin.

An additional 2.6-hr 3.5-kHz PDR and SCS survey was conducted on approaching the site (JR survey line S10; Fig. **F24**) from west to east, crossing line S7 at about shotpoint 380. The ship's average speed was 5.8 kt. The water gun was triggered at a shot interval of 12 s, equivalent to ~36 m at 5.8 kt. An asymmetric basin structure with a steeper basement reflector on the eastern side is revealed in the S10 seismic profile (Fig. **F25**). No distinct reflector signals can be found in the basin, implying that the sediment is relatively homogeneous. Site 1162 was located ~5.8 km west of the prospectus site AAD-39a at a position corresponding to shotpoint 214 of seismic profile S10. The scattering of basement signals, ranging from 7.55 to 7.73 s in two-way traveltime, indicates a complicated variation of basement relief in the vicinity of Site 1162. Sediment cover was estimated to be between 220 and 400 m (Fig. **F25**). We washed through 333.2 m of sediment in Hole 1162A before basement was reached, whereas Hole 1162B, about 200 m north, penetrated 348.4 m of sediment.

F23. Cataclasite with ultracataclasite and a few narrow shear zones, p. 38.
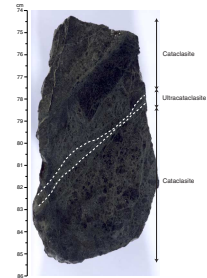
F24. Track chart of the SCS survey line S10 and part of S7, p. 39.
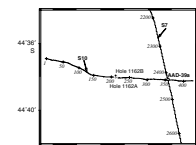
F25. SCS profile of line S10 from shotpoints 1 to 428, p. 40.
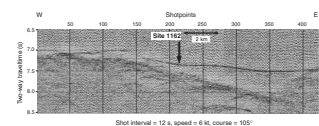
SEDIMENTS

Hole 1162A

One wash core was recovered from Hole 1162A (Core 187-1162A-1W; 0.0–333.2 mbsf). Drilling-induced pellets of predominantly gray with minor brown siliceous clay are in Section 187-1162A-1W-1, 0–85 cm. The pellets range in size from submillimeter to ~1 cm and are poorly sorted but normally graded over this interval as a result of agitation in the core barrel. The ratio of dark gray to medium brown pellets is ~20:1. Embedded in the lowermost 20 cm of this interval are several tube casts up to 10 cm long and a centimeter in diameter with elliptical cross sections. Also in this interval are a couple of centimeter-sized clasts of black chert. Interbedded dark gray and dark brown densely packed siliceous clay is in Section 187-1162A-1W-1, 85–134 cm. Intervals are a few centimeters thick with sharp but irregular contacts. A smear slide from the lowermost layer contains abundant gray clay and ~2%, 4- to 10-µm carbonate rhombs. From 135 to 136.5 cm in Section 187-1162A-1W-1 is a distinct change to reddish gray siliceous clay with sharp but irregular contacts. Below Section 187-1162A-1W-1, 135 cm, and continuing through Section 1W-2, 44 cm, is light brownish red clay with rare lenses (<2 cm across) of deep-red clay. At Section 187-1162A-1W-2, 44 cm, is a sharp drilling-disturbed contact and a change to densely packed, very stiff, red siliceous clay. A smear slide from the lower part of this section looks identical to the smear slide from the gray clay above except in the color of the clay. The pieces in the core catcher from this core are predominantly red clay with a few discontinuous lenses of light brown clay. These lenses also contain disseminated submillimeter-sized Mn oxide clasts.

Hole 1162B

This core contains predominantly greenish gray clay and a breccia with abundant altered basaltic clasts. From the top of Section 187-1162B-1W-1 to Section 1W-2, 24 cm, is a slurry of greenish gray siliceous clay. In Section 187-1162B-1W-1 several intervals (30–45, 64–76, 100–105, 111–116, and 135–147 cm) are thick biscuits of more densely packed, less drilling-disturbed clay. Intervals between these biscuits are soupy. Except for the interval between 30 and 45 cm, the upper 56 cm of Section 187-1162B-1W-1 is a normally graded, poorly sorted slurry of drilling-induced gray and light brown clay pellets (ratio of gray to brown >20:1). The interval from 30 to 45 cm in Section 187-1162B-1W-1 is brownish green. From 24 to 75 cm in Section 187-1162B-1W-2 is densely packed, stiff, greenish gray siliceous clay with thin (<1 cm) layers and lenses of dark green clay. From 0 to 52 cm in Section 187-1162B-1W-3 is severely drilling-disturbed greenish gray clay with a few pieces of dark green chert and a couple of silicified tube casts near the bottom of the interval. From 52 to 60 cm is dark brown siliceous clay; from 60 to 78 cm is layered dark gray and medium gray densely packed clay. The contacts in this interval are sharp but irregular. Below Section 187-1162B-1W-3, 78 cm, and throughout Section 1W-CC is a clay- and carbonate-cemented altered basaltic breccia. A smear slide from Section 187-1162B-1W-2, 60 cm, contains abundant siliceous microfossil fragments (unlike the sediment from Core 187-1162A-1W) but none of the carbonate rhombs present in the wash core from Hole 1162A.

GEOCHEMISTRY

Introduction

Two holes at Site 1162 penetrated ~18-Ma crust, 37 km south of the dying rift/transfer zone sampled at Site 1161 in Zone A. In both Holes 1162A and 1162B, we encountered dolomite-cemented breccia containing highly altered basalt clasts along with several other lithologies. Alteration was so pervasive that only one glass from Hole 1162B was available for major and trace element analysis by ICP-AES (Table T3). Two samples of the carbonate cement were also analyzed by ICP-AES to establish whether this authigenic material is high-Mg calcite or dolomite.

Hole 1162B

The single analyzed glass sample from Site 1162 contains ~10% spherulites. Its composition is typical for Zone A, Pacific-type basalt. It contains ~7.7 wt% MgO; Y and Ba are slightly high and Na_2O and CaO/Al_2O_3 are relatively low, but, without additional data, this sample is not considered to be distinct from normal Zone A compositions.

Temporal Variations

Our limited Site 1162 data show no convincing evidence for temporal change beneath the Zone A spreading axis. Rather, the Site 1162 basalt glass documents a prior period of seafloor accretion similar to that occurring today (Figs. F26, F27).

Mantle Domain

The Zr/Ba vs. Ba (Fig. F28A) and Na_2O/TiO_2 vs. MgO (Fig. F28B) systematics of Hole 1162B glass indicate a Pacific-type mantle source. The glass composition lies slightly outside the tip of the Pacific-type mid-ocean-ridge basalt field with lower Zr/Ba than 0- to 7-Ma Pacific-type lavas and Ba at the high end of the 0- to 7-Ma range. Several samples from Leg 187 sites have this ambiguous trait, plotting outside both Pacific- and Indian-type fields on this diagram in a field that we have previously termed Transitional Pacific (see "Barium and Zirconium," p. 13, in the "Leg Summary" chapter). Nonetheless, we believe this sample to be unequivocally Pacific type because it is conceivably on a mixing trend toward the propagating rift lavas and/or has formed by slightly lower degrees of melting. The high Ba content could also result from the necessary inclusion of spherulitic material within the analyzed sample. Slightly lower Ba (i.e., glass without spherulites) would move this data point into the Pacific-type field. The Na_2O/TiO_2 diagram clearly indicates a Pacific-type source, well within the range of Segments A2 and A3 glasses.

T3. Compositions of basalts from Site 1162, p. 46.

F26. Major element compositions vs. MgO for Hole 1162B basalt glass, p. 41.
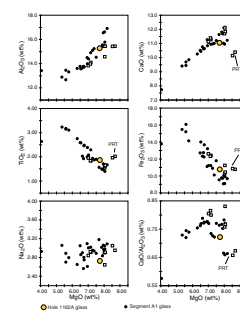
F27. Trace element compositions vs. MgO for Hole 1162B basalt glass, p. 42.
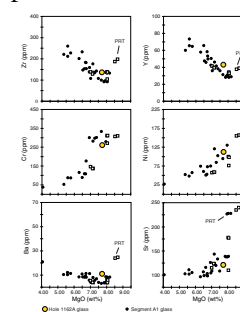
F28. Variations of Zr/Ba vs. Ba and Na_2O/TiO_2 vs. MgO for Hole 1162B basalt glass, p. 43.
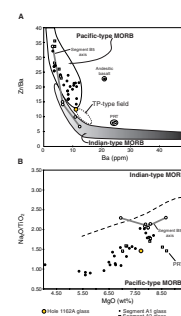
REFERENCES

Alt, J.C., Laverne, C., Vanko, D.A., Tartarotti, P., Teagle, D.A.H., Bach, W., Zuleger, E., Erzinger, J., Honnorez, J., Pezard, P.A., Becker, K., Salisbury, M.H., and Wilkens, R.H., 1996. Hydrothermal alteration of a section of upper oceanic crust in the eastern equatorial Pacific: a synthesis of results from Site 504 (DSDP Legs 69, 70, and 83, and ODP Legs 111, 137, 140, and 148.) *In* Alt, J.C., Kinoshita, H., Stokking, L.B., and Michael, P.J. (Eds.), *Proc. ODP, Sci. Results,* 148: College Station, TX (Ocean Drilling Program), 417–434.

Ramsay, J.R., and Huber, M.I., 1987. *The Techniques of Modern Structural Geology* (Vol. 2): *Folds and Fractures:* London (Academic).

Figure F1. Photomicrograph in plane-polarized light of Sample 187-1162A-2R-1 (Piece 1, 1–3 cm; see "Site 1162 Thin Sections," p. 24), showing coalesced spherulite pseudomorphs in the chilled margin of a metabasalt that has been completely replaced by a mixture of chlorite and actinolite.
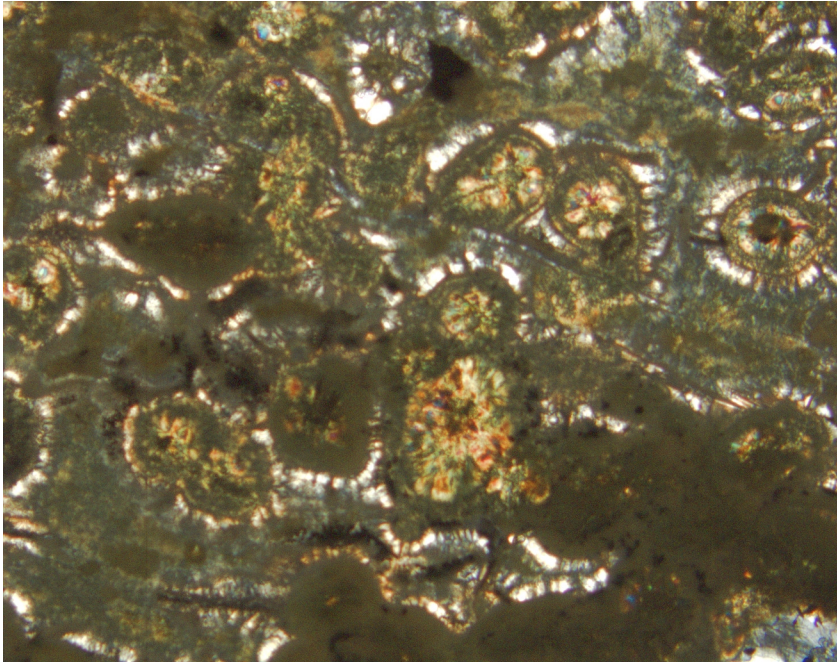
2 mm

Figure F2. Photomicrograph, with crossed polars, of Sample 187-1162A-2R-1 (Piece 1, 1–3 cm; see "Site 1162 Thin Sections," p. 24), showing an oval plagioclase xenocryst with melt inclusions in the altered glass of a metabasalt. A quartz vein runs from the top left to center bottom.
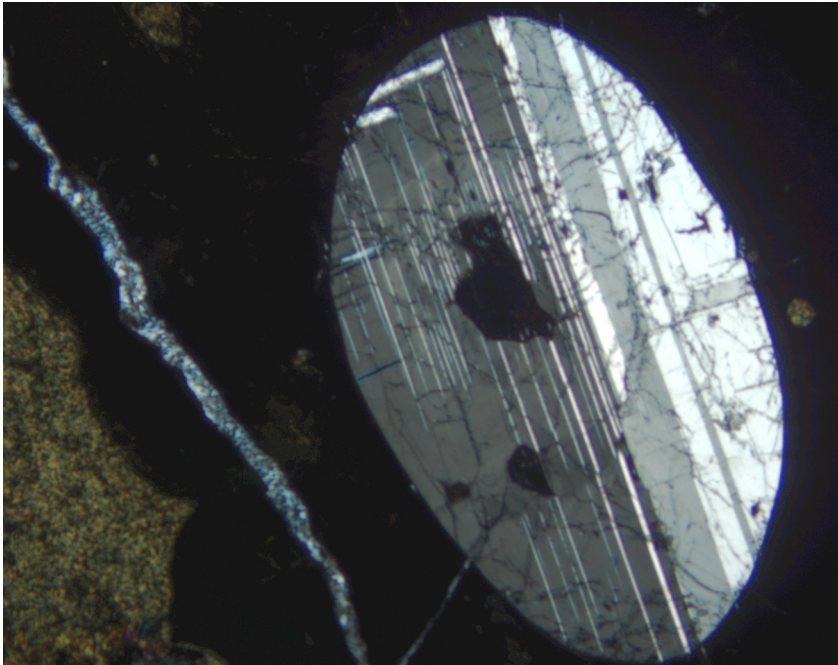
4 mm
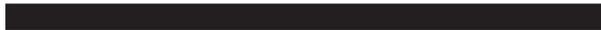
Figure F3. Photomicrograph, with crossed polars, of Sample 187-1162A-2R-1 (Piece 1, 1–3 cm) (see **"Site 1162 Thin Sections,"** p. 24), showing quench-crystal overgrowths on the edge of an oval plagioclase xenocryst in Figure **F2**, p. 17.
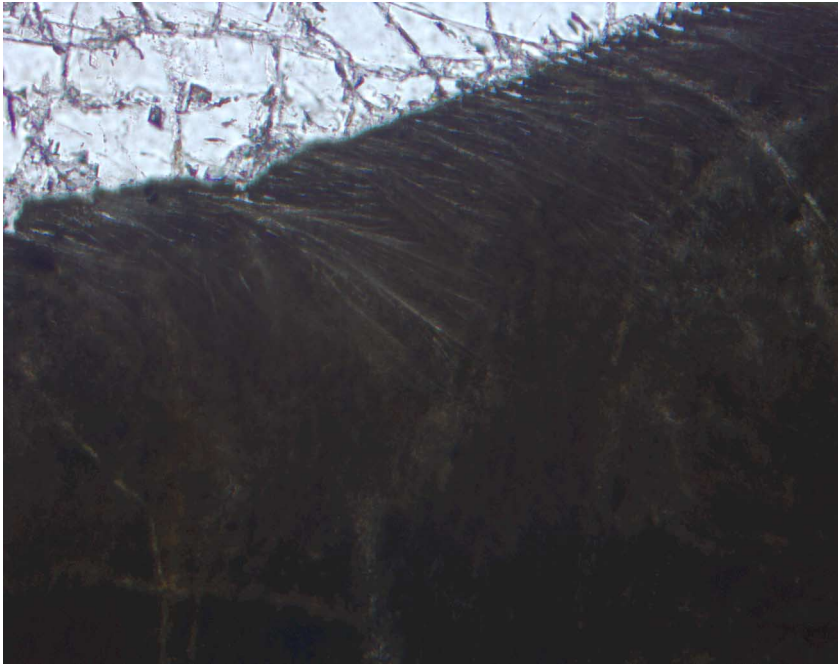
0.5 mm

Figure F4. Photomicrograph, with crossed polars, of Sample 187-1162A-5R-1 (Piece 15, 73–75 cm) (see **"Site 1162 Thin Sections,"** p. 27), showing part of a plagioclase glomerocryst in altered metabasalt. One original crystal (occupying most of the field of view) is now four separate grains. Oscillatory zoning can still be seen within the three grains that make up the top left of the field of view, but these grains have different extinction angles. The dark area (top left) is clay replacing olivine.
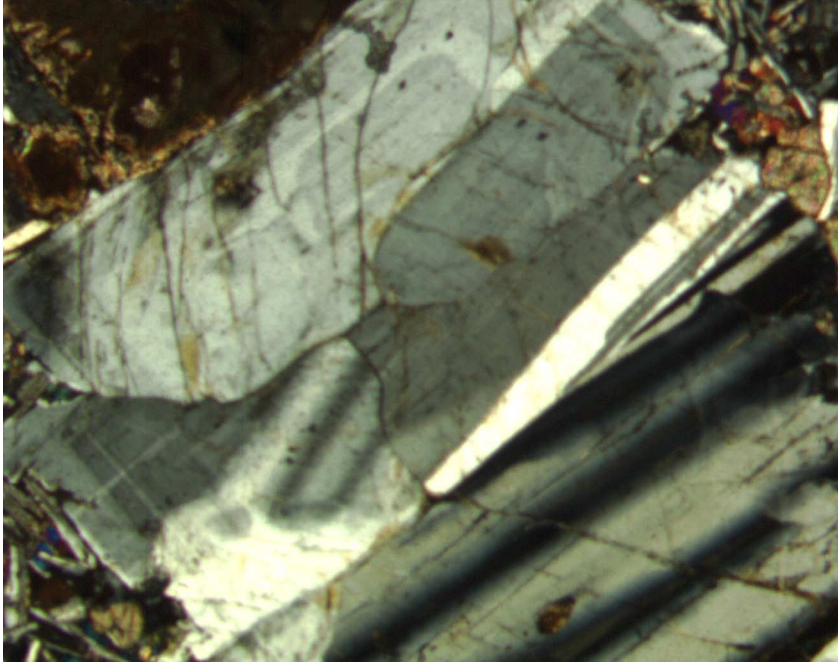
2 mm
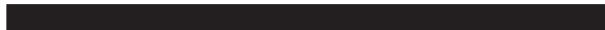
Figure F5. Photomicrograph, with crossed polars, of Sample 187-1162A-5R-1 (Piece 7, 25–28 cm) (see **"Site 1162 Thin Sections,"** p. 26), showing an olivine phenocryst in metadiabase that is totally replaced by concentric rings of highly birefringent talc and opaque minerals, with cummingtonite? (C, center). Actinolite (A, lower right) has replaced matrix clinopyroxene.
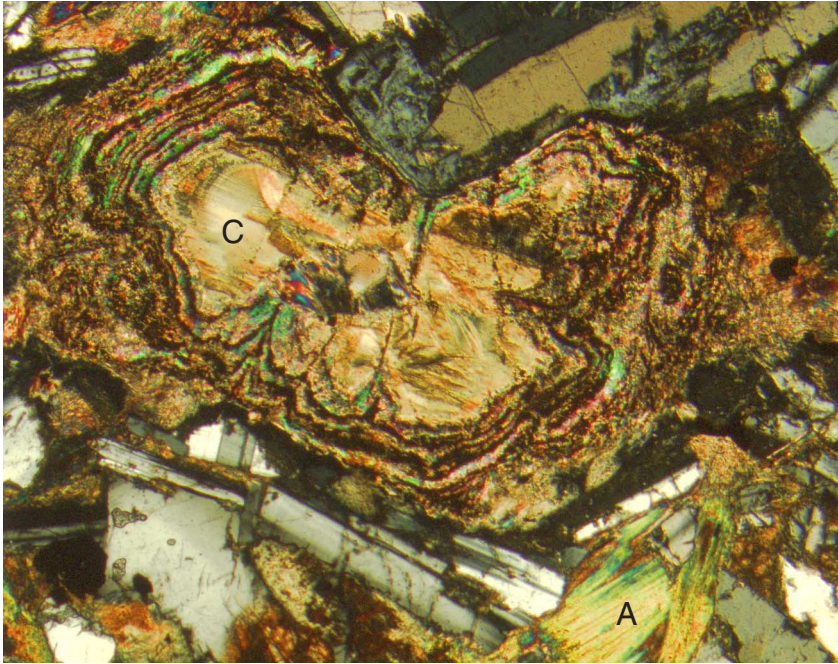
2 mm

Figure F6. A. Photomicrograph in plane-polarized light of Sample 187-1162A-5R-1 (Piece 7, 25–28 cm) (see "Site 1162 Thin Sections," p. 26), showing actinolite bundles (green) with chlorite (C; patchy brown/black, below and right) after clinopyroxene in metagabbro. **B.** Photomicrograph, with crossed polars, of the same view.

A

B
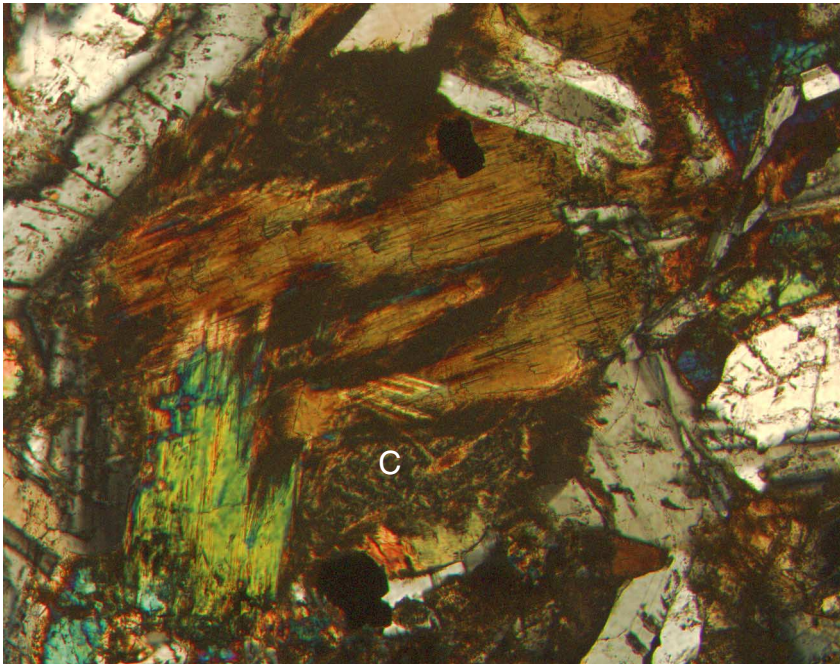
1 mm

Figure F7. Photomicrograph in plane-polarized light of Sample 187-1162B-3R-1 (Piece 22, 116–120 cm) (see "Site 1162 Thin Sections," p. 30), a dolomite-cemented basalt breccia. An altered basaltic clast (bottom) has a chilled margin that has been replaced by brown palagonite (P, top of clast). Dolomite crystals along the edge of the clast are larger and elongate perpendicular to the clast; these larger crystals have fewer impurities than those farther into the matrix. This can be seen as a clear rim in hand specimen.
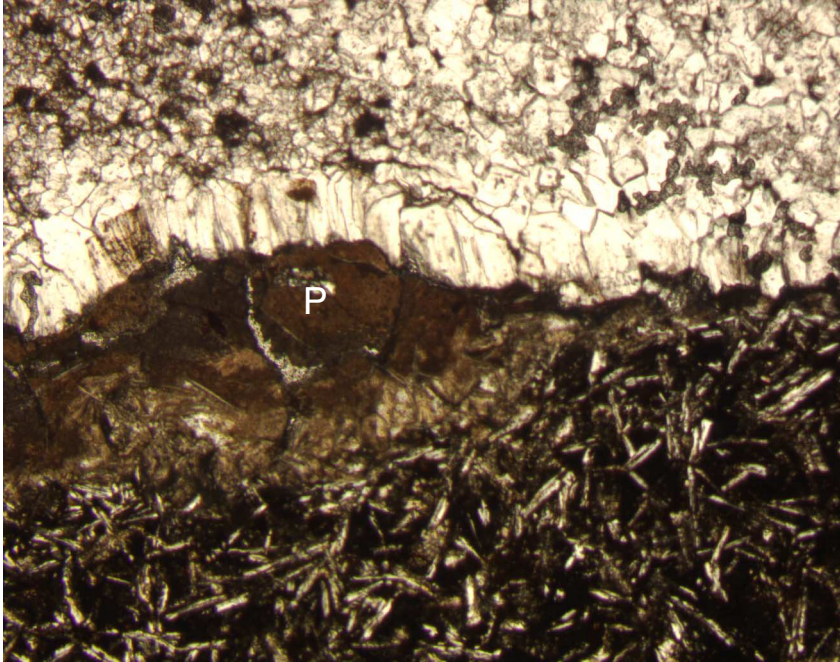
2 mm

Figure F8. Photomicrograph in plane-polarized light of Sample 187-1162B-3R-1 (Piece 22, 116–120 cm) (see "Site 1162 Thin Sections," p. 30), showing a palagonite clast in a dolomite-cemented basalt breccia with characteristic concentric zoning partially replaced by crystalline dolomite of the groundmass.

Palagonite

Dolomite replacing palagonite
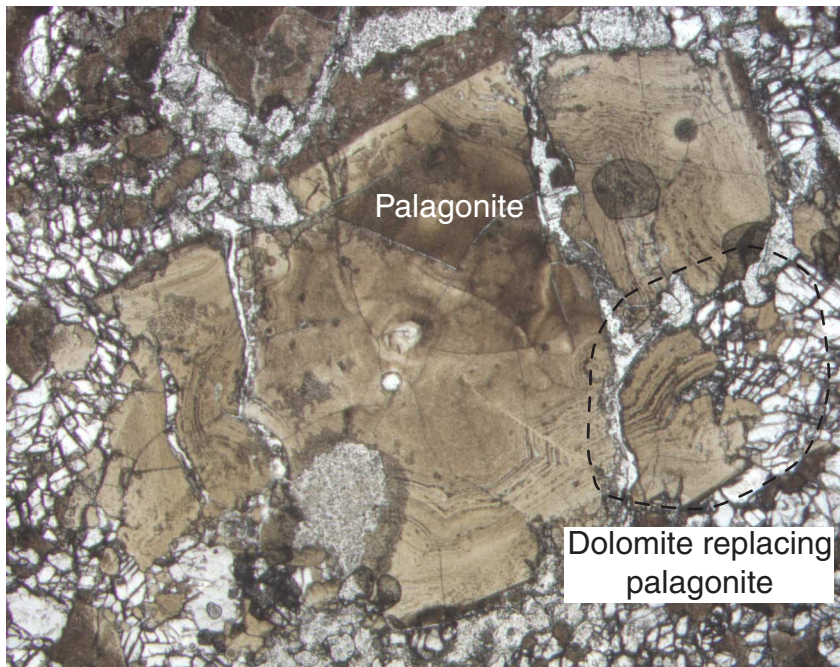
2 mm

Figure F9. Photograph of interval 187-1162A-5R-1, 54–60 cm, showing a highly altered piece of moderately plagioclase-olivine phyric basalt. Note the centimeter-sized plagioclase megacryst.
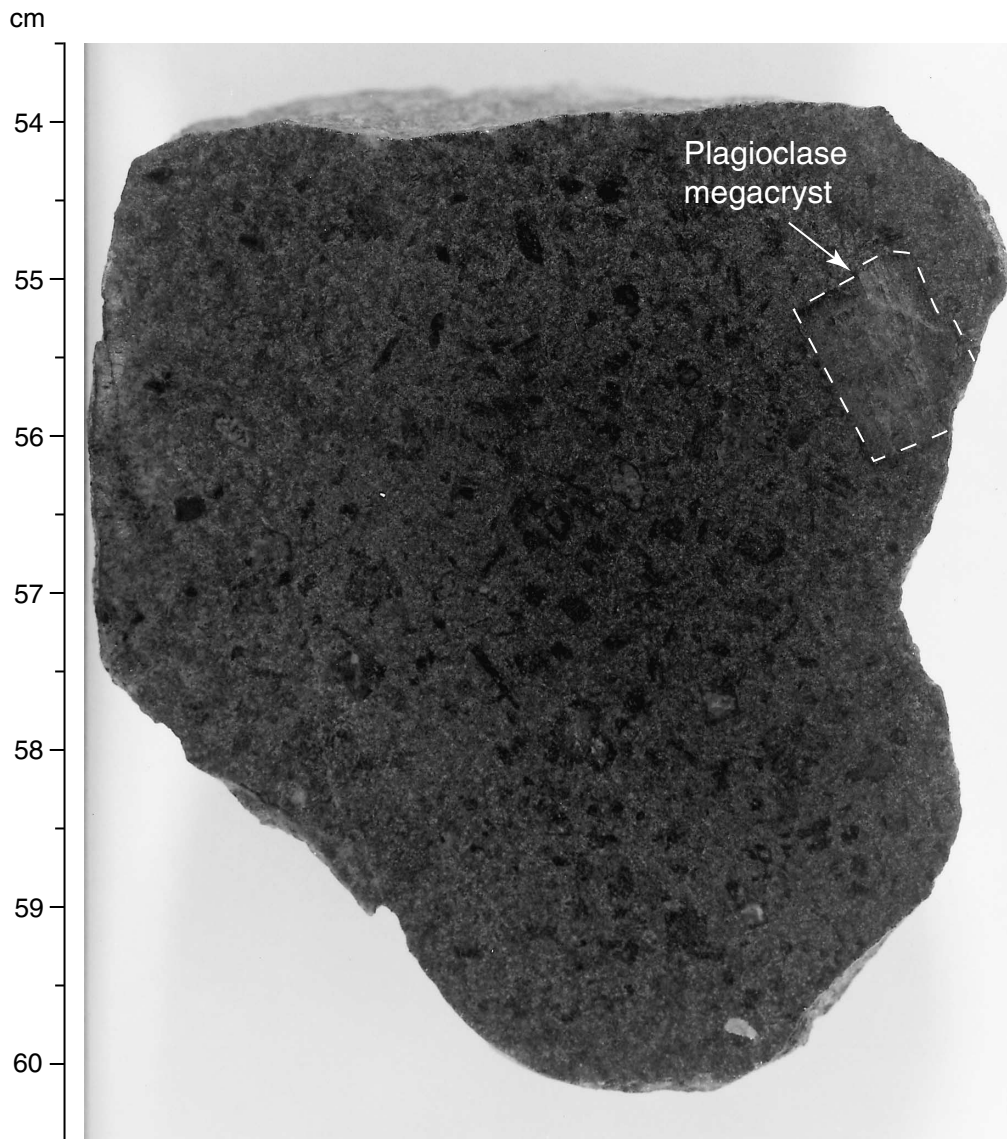
Figure F10. Photomicrograph in plane-polarized light of Sample 187-1162A-5R-1, 73–75 cm (see **"Site 1162 Thin Sections,"** p. 27), showing an olivine phenocryst replaced by opaque minerals and Fe oxyhydroxides, rimmed by a mixture of chlorite and talc.
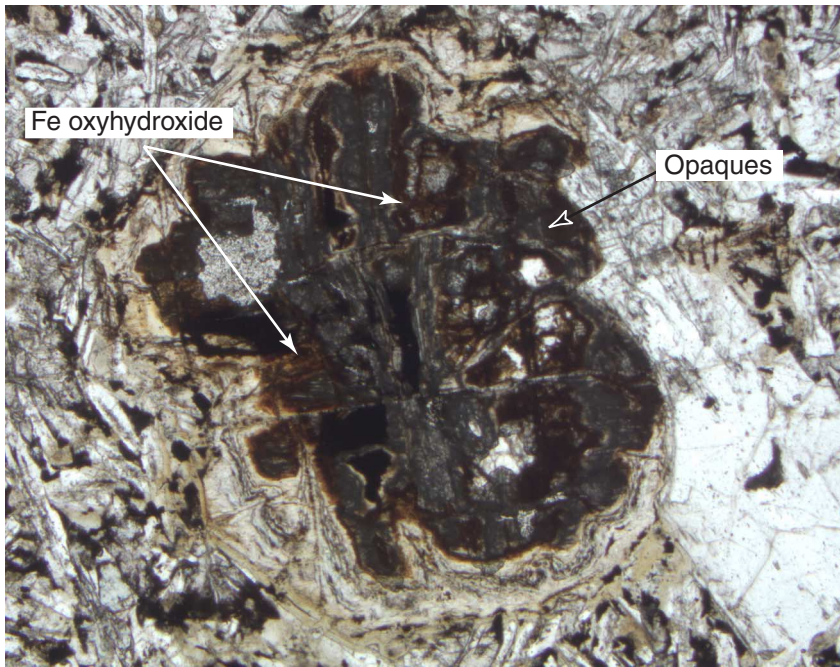
2 mm

Figure F11. Photomicrograph, with crossed polars, of Sample 187-1162A-5R-1, 73–75 cm (see **"Site 1162 Thin Sections,"** p. 27), showing an olivine microphenocryst totally replaced by chlorite, talc, and opaque minerals.
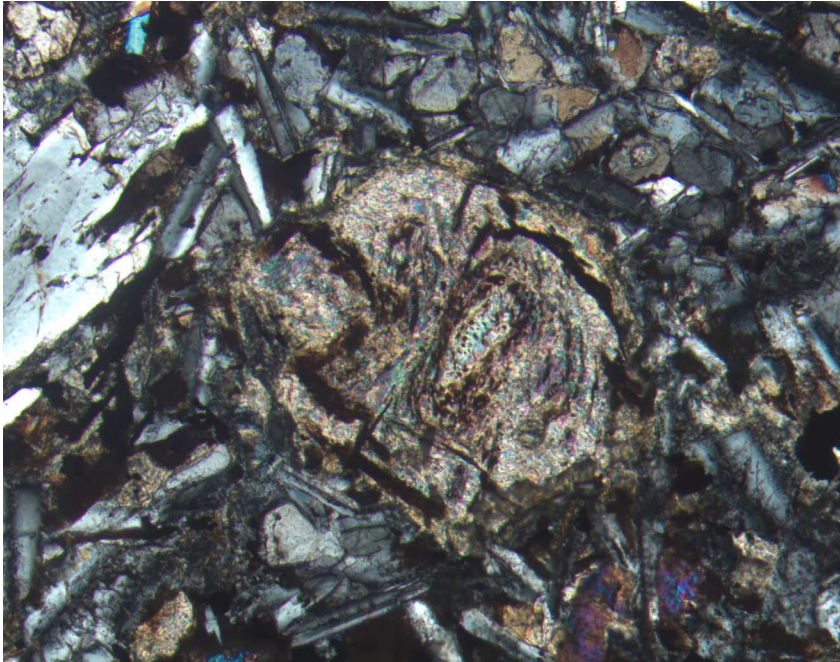
1 mm

Figure F12. Photomicrograph in plane polarized light of Sample 187-1162A-5R-2, 55–60 cm (see **"Site 1162 Thin Sections,"** p. 28), showing replacement of groundmass clinopyroxene by chlorite. Note the fresh clinopyroxene (upper right corner).
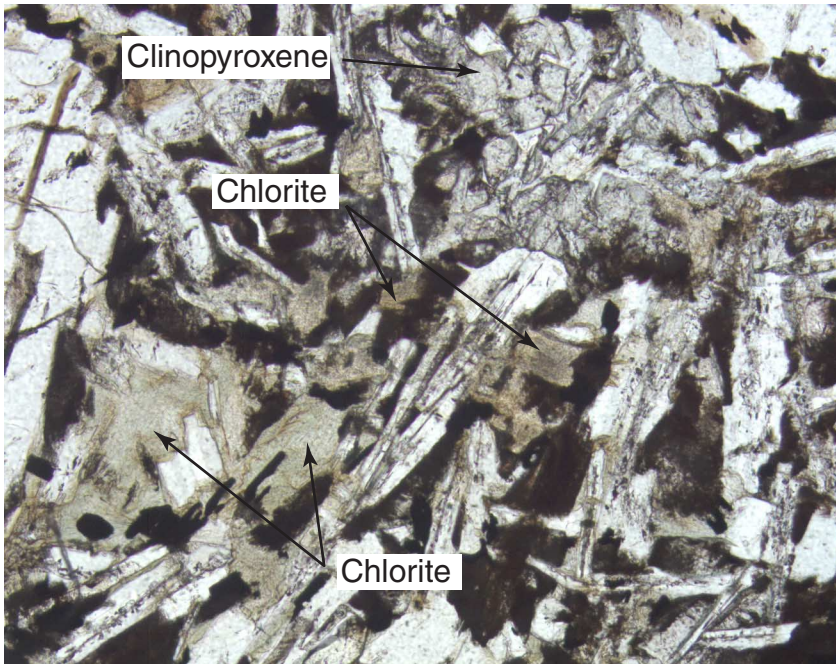
1 mm

Figure F13. Photograph of interval 187-1162A-5R-1, 24–30 cm, showing a highly altered metadiabase.
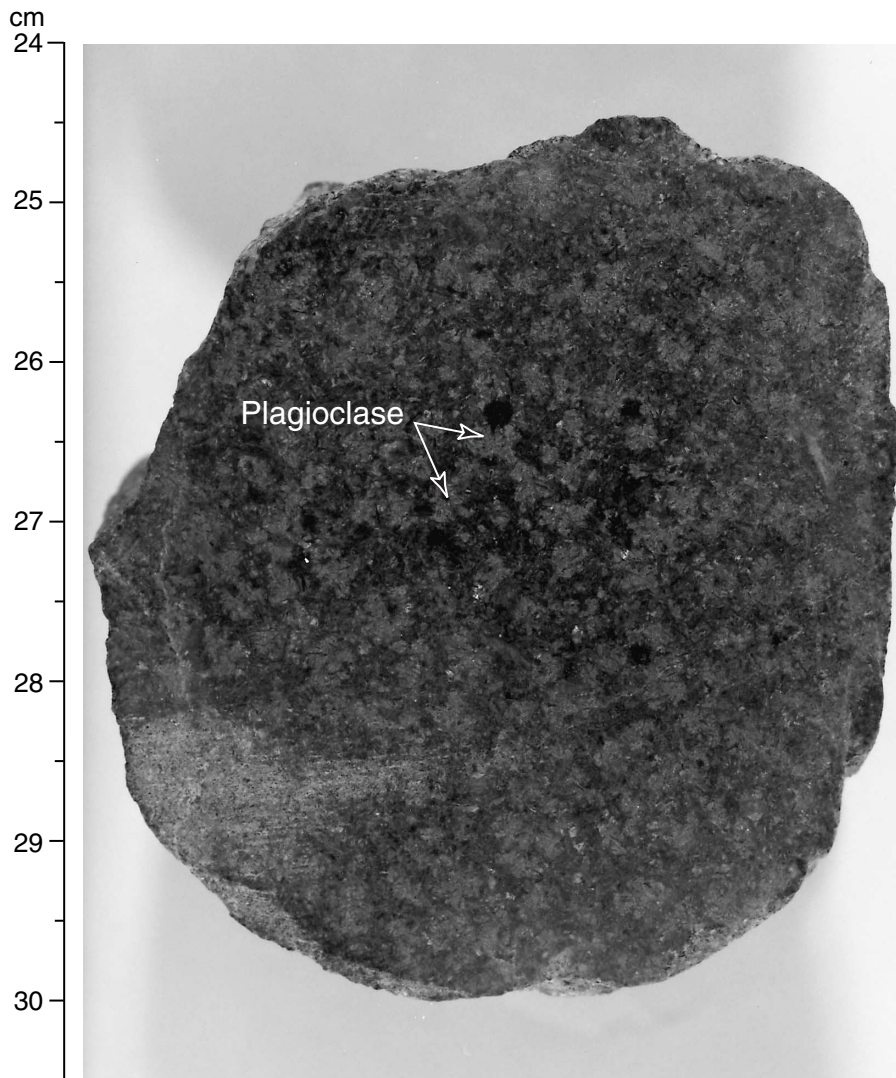
Figure F14. Photomicrograph, with crossed polars, of Sample 187-1162A-5R-1, 25–28 cm (see "Site 1162 Thin Sections," p. 26), showing chlorite and actinolite replacing clinopyroxene in metadiabase.
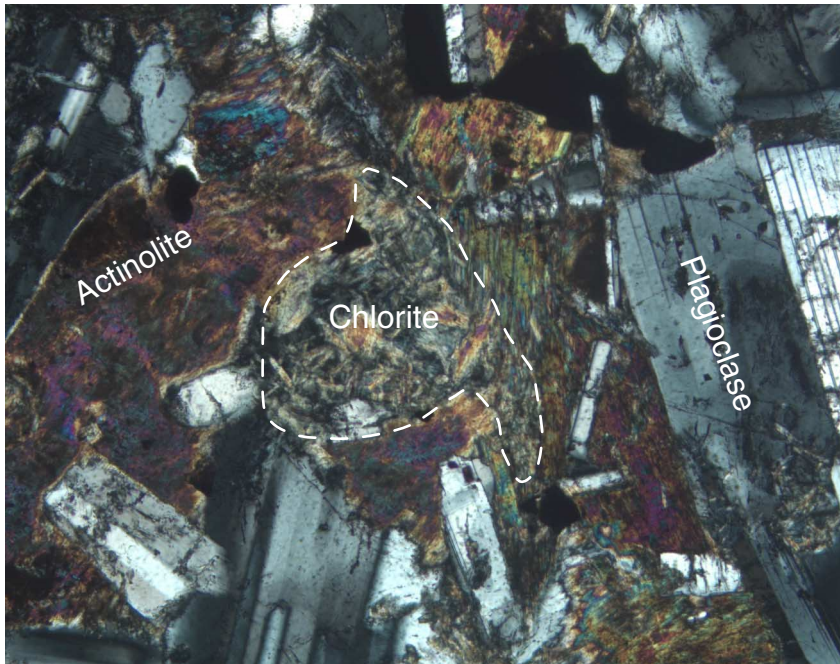
1 mm
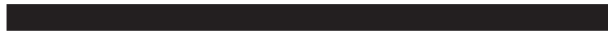
Figure F15. Photomicrograph, with crossed polars, of Sample 187-1162A-5R-1, 25–28 cm (see **"Site 1162 Thin Sections,"** p. 26), showing an olivine phenocryst replaced by cummingtonite and surrounded by concentric layers of talc and opaque minerals. Note the fibrous actinolite replacing clinopyroxene.
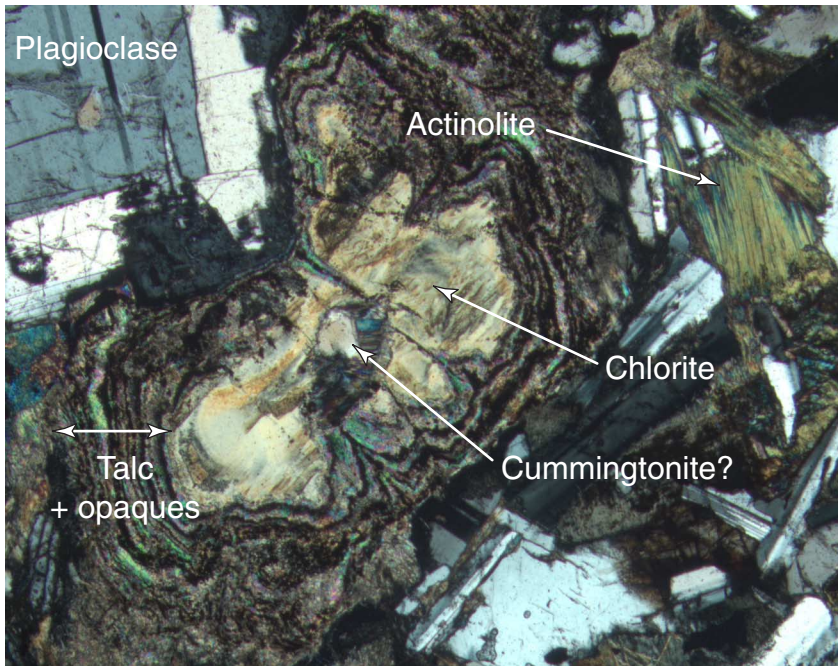
2 mm

Figure F16. Photomicrograph, with crossed polars, of Sample 187-1162A-2R-1, 1–3 cm (see **"Site 1162 Thin Sections,"** p. 24), showing the spherulitic zone in metabasalt from Hole 1162 (Unit 1) in which spherulites and mesostasis have been replaced by actinolite. Note the curved vein of recrystallized quartz that shows strain extinction and preferred orientation of crystallographic axes.
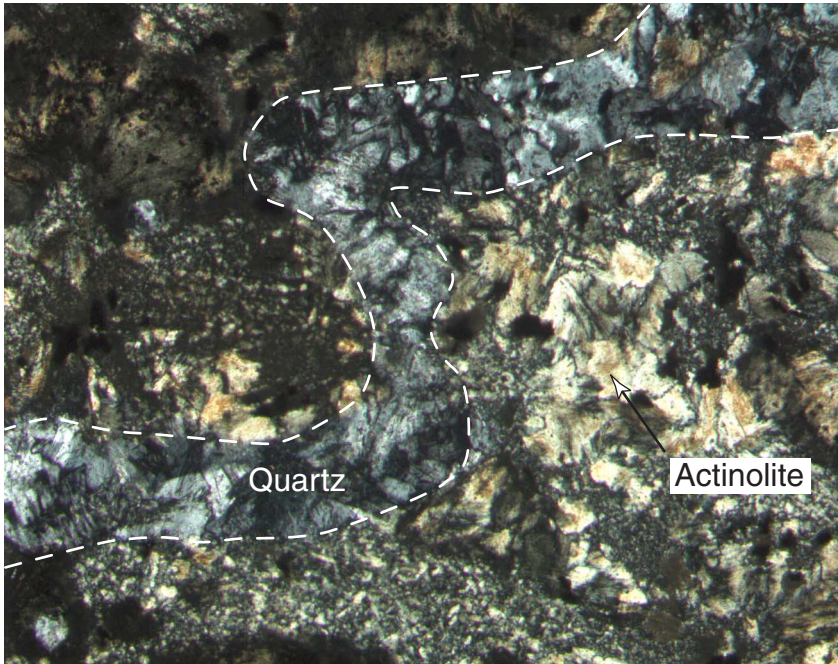
1 mm

Figure F17. Photograph of interval 187-1162A-4R-1, 74–86 cm, showing a basaltic cataclasite with a conjugate shear plane set.
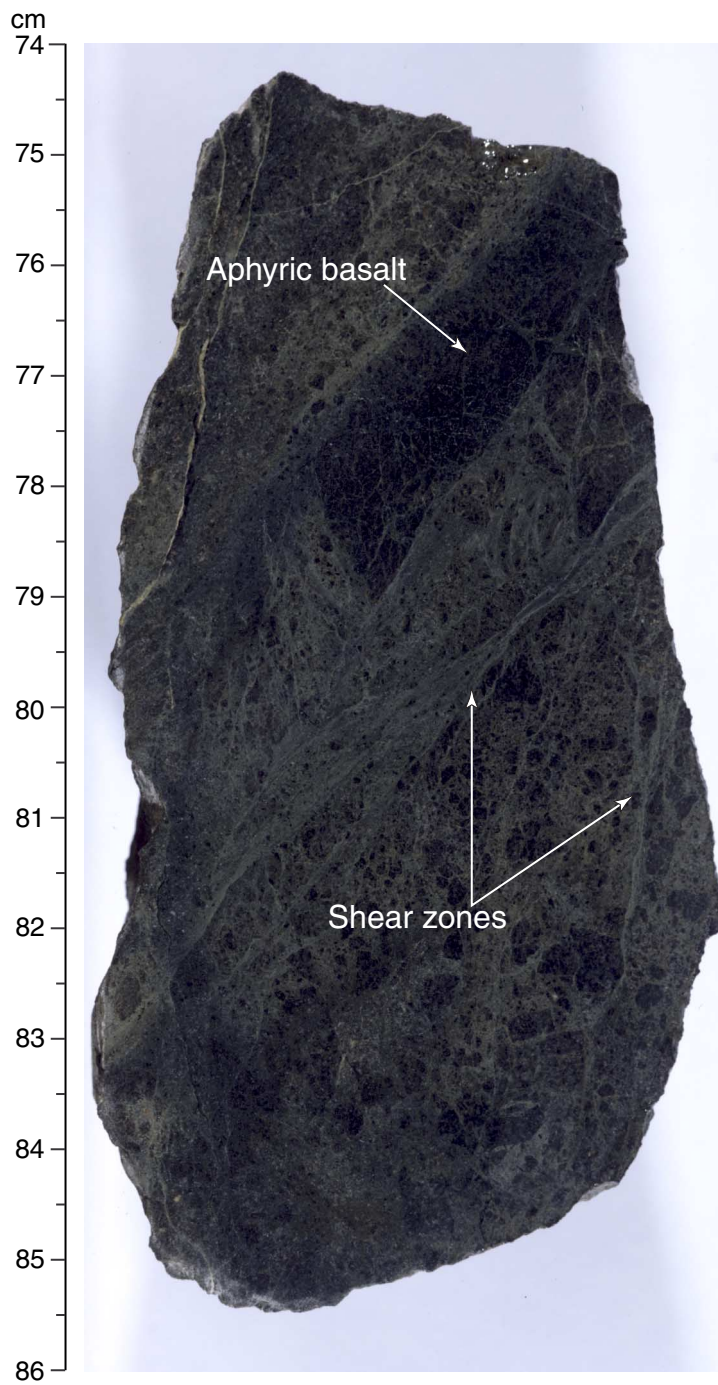
Figure F18. Photograph of interval 187-1162B-5R-1, 79–85 cm, showing a highly to very highly altered piece of sparsely phyric plagioclase-olivine basalt. Note the quenched margin at the bottom of the piece.
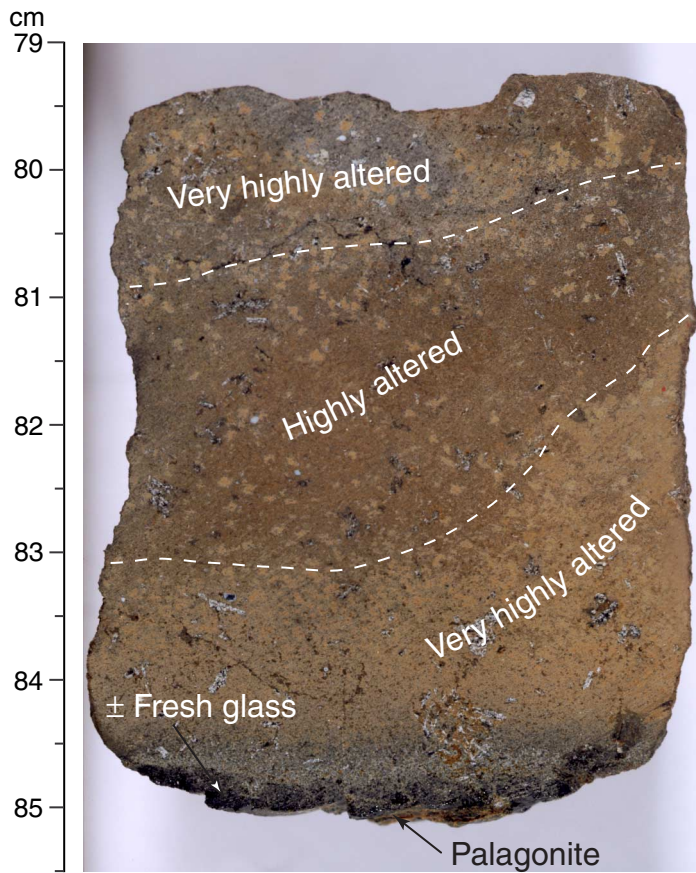
Figure F19. Photograph of interval 187-1162B-5R-1, 41–49 cm, showing the dolomite-cemented basalt breccia. The large clasts are highly to very highly altered basalt, dissected by 1- to 2-mm-wide veins of crystalline dolomite. Palagonite clasts have distinct concentric layers. Note that the breccia matrix consists of two generations: early pale pink dolomite, cut by later veins of crystalline dolomite. Mn oxide spots are associated only with the first-generation dolomite.
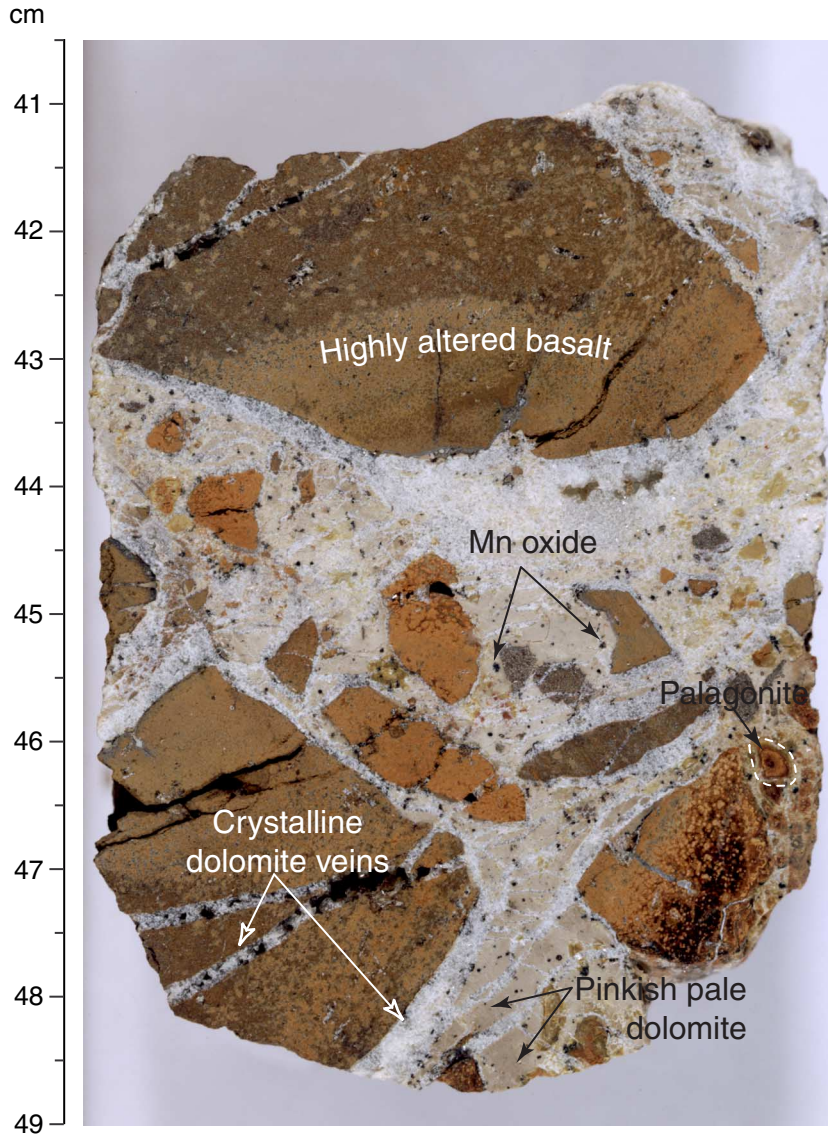
Figure F20. Photomicrograph in plane-polarized light of Sample 187-1162B-2R-1, 59–62 cm (see **"Site 1162 Thin Sections,"** p. 29), showing groundmass clinopyroxene and plagioclase replaced by smectite and Fe oxyhydroxide.
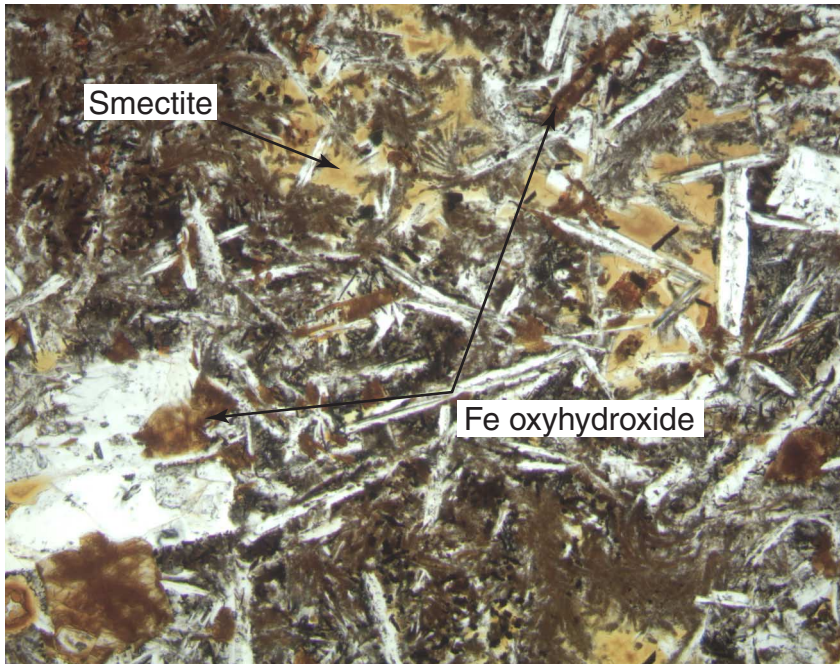
Figure F21. Photograph of interval 187-1162B-4R-1, 91–103 cm, showing dolomite-cemented basalt breccia with completely altered basalt fragments that have large open shrinkage cracks caused by contraction during drying of the core. This reflects the high abundance of clay replacing the groundmass. Note the pillow basalt fragment (center), having the typical V-shaped form and remnants of a chilled margin.
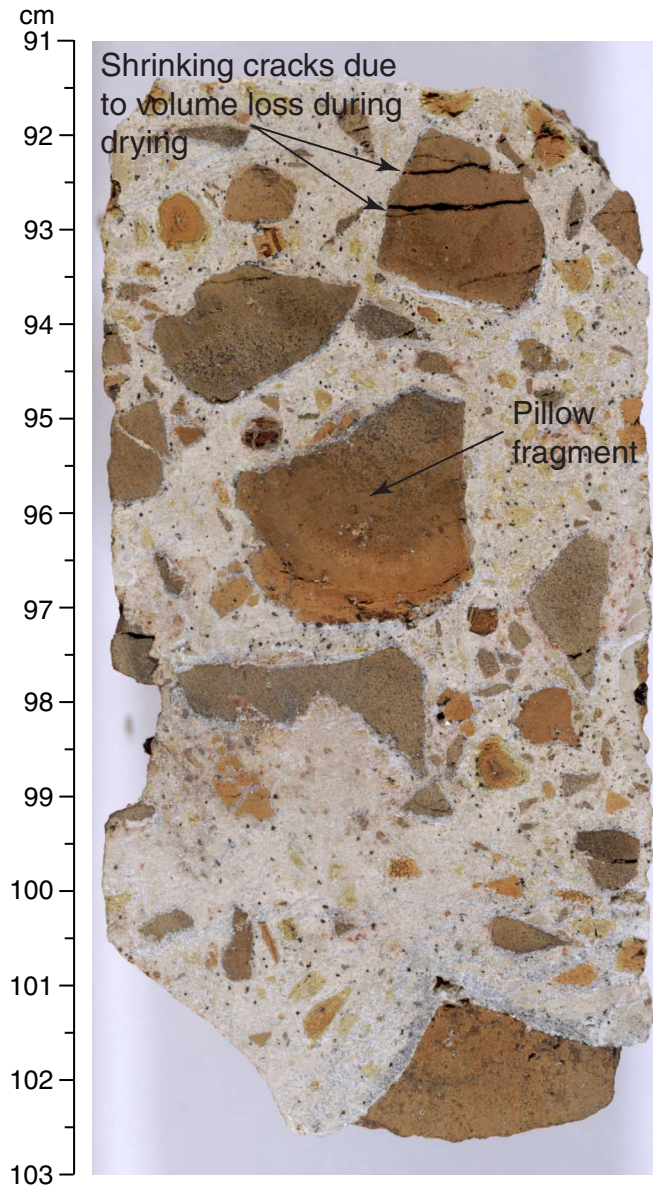
Figure F22. Photomicrograph in plane-polarized light of Sample 187-1162B-2R-1, 59–62 cm (see "Site 1162 Thin Sections," p. 29), showing a crystalline dolomite vein cutting both a highly altered basalt clast and an impure first-generation dolomite.
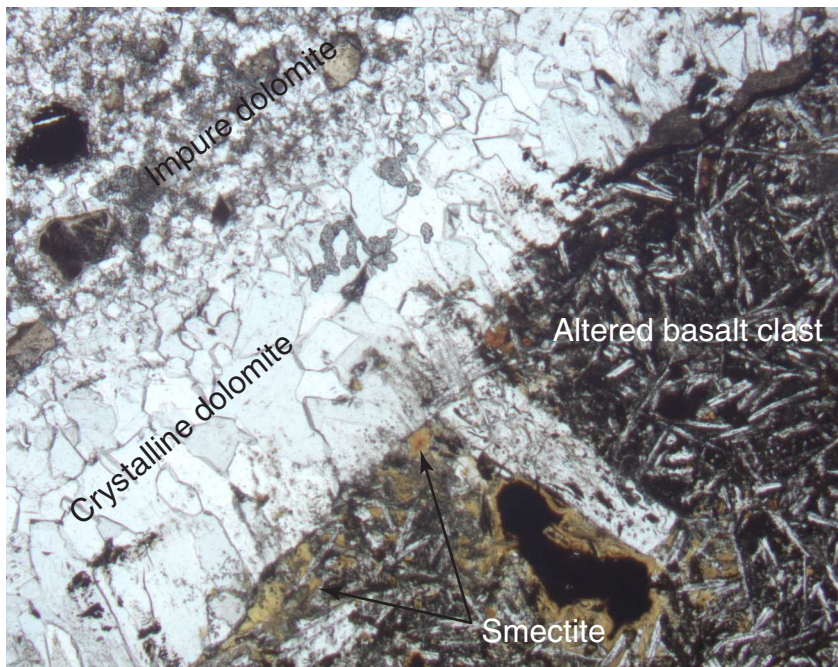
2 mm

Figure F23. Photograph of Section 187-1162A-4R-1 (Piece 13, 74–86 cm), showing cataclasite with ultracataclasite and a few narrow shear zones.
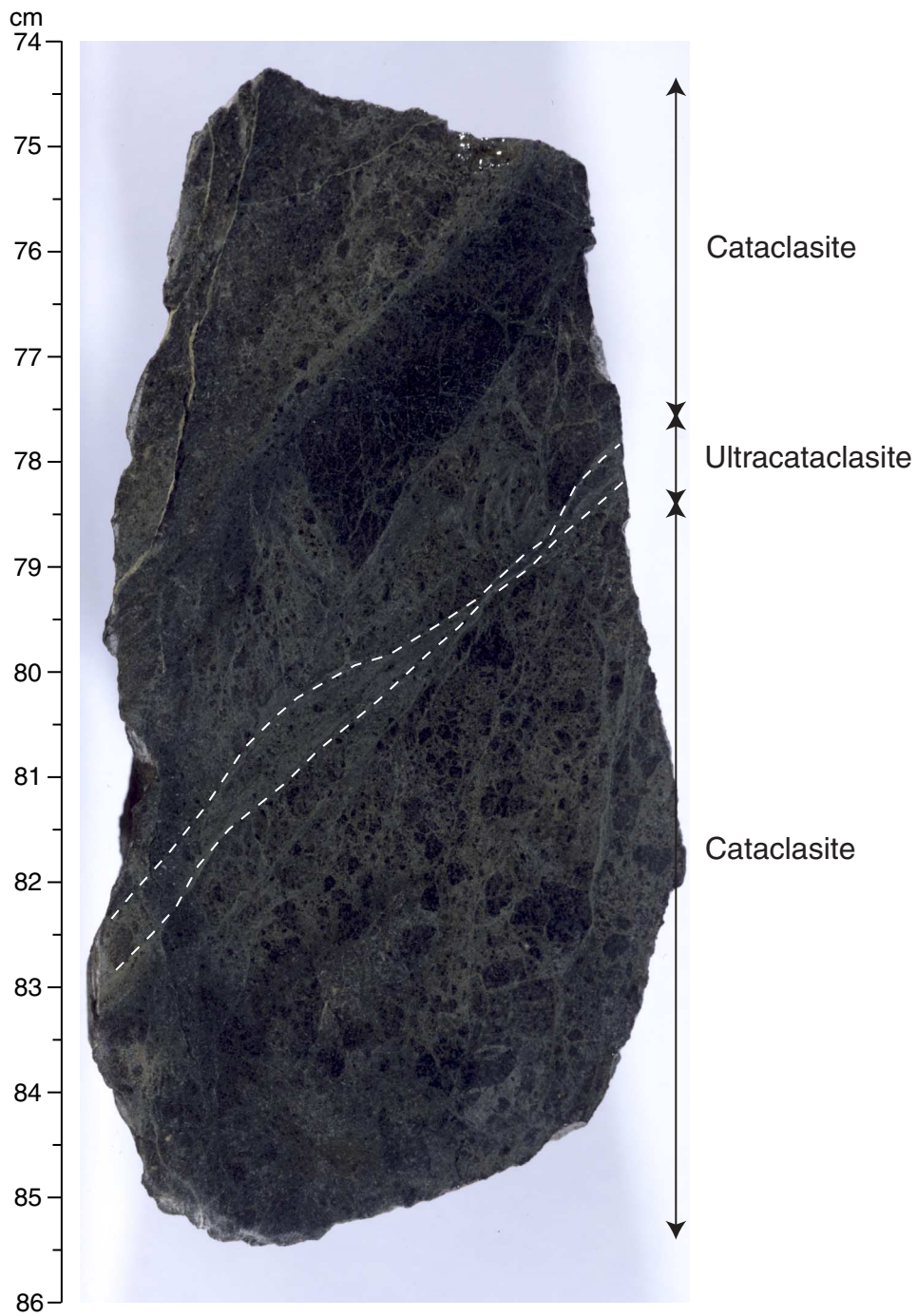
Figure F24. Track chart of the single-channel seismic survey line S10 and part of S7. Crosses = 50-shot intervals for line S10 and 100-shot intervals for line S7. Holes 1162A and 1162B (solid circles) are near shot-point 214, ~5.8 km west of the prospectus site AAD-39a.
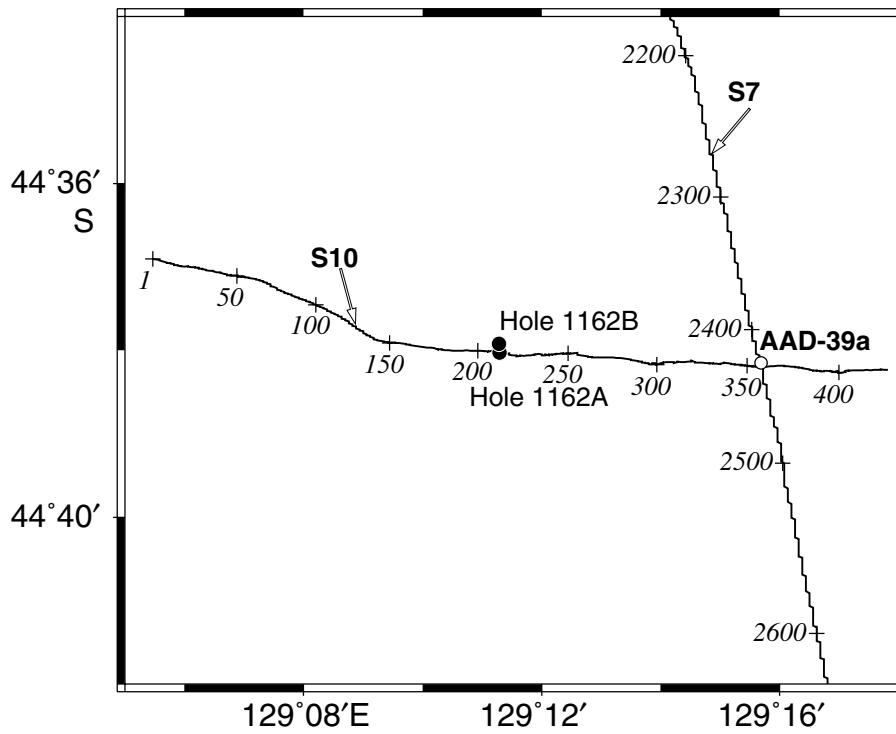
Figure F25. A single-channel seismic profile of line S10 from shotpoints 1 to 428. The large arrow marks the position of Site 1162 near shotpoint 214. The seafloor at Site 1162 corresponds to 7.33 s in two-way traveltime.

Shot interval = 12 s, speed = 6 kt, course = 105°
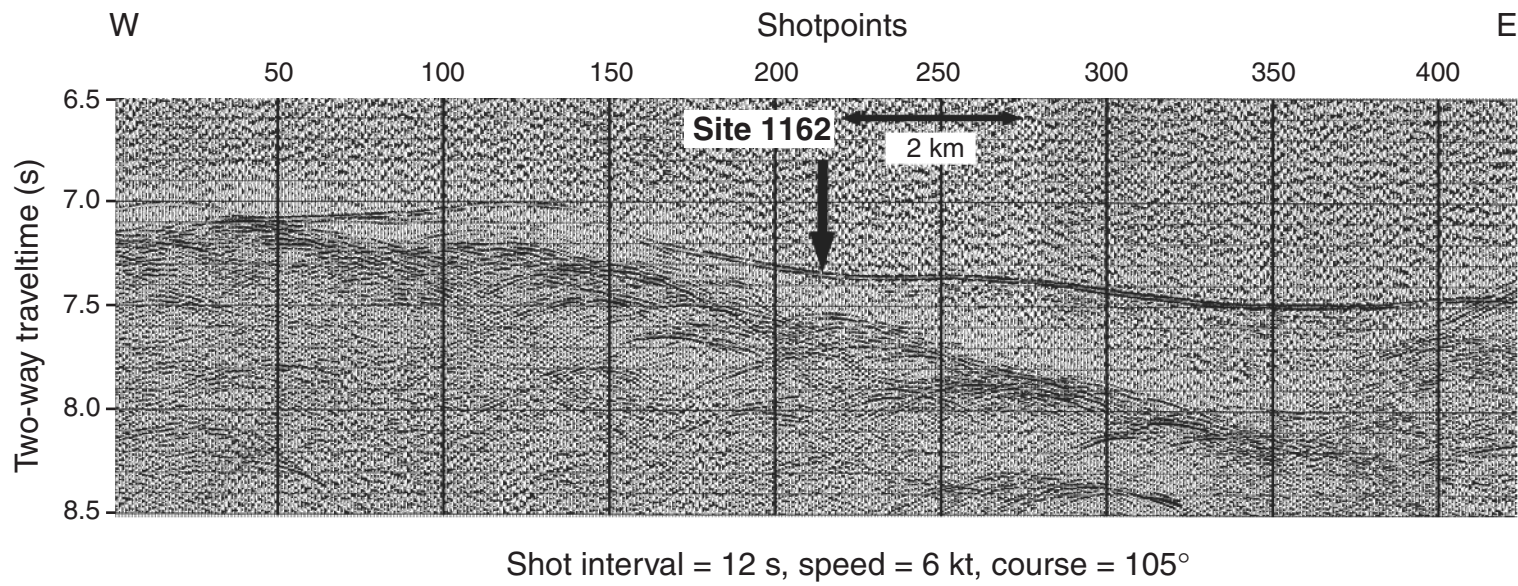
Figure F26. Major element compositions vs. MgO for Hole 1162B basalt glass compared with Segment A1 and A2 glass from Zone A. Only the average of ICP-AES analyses reported in Table T3, p. 46, are plotted. PRT = propagating rift tip lavas.
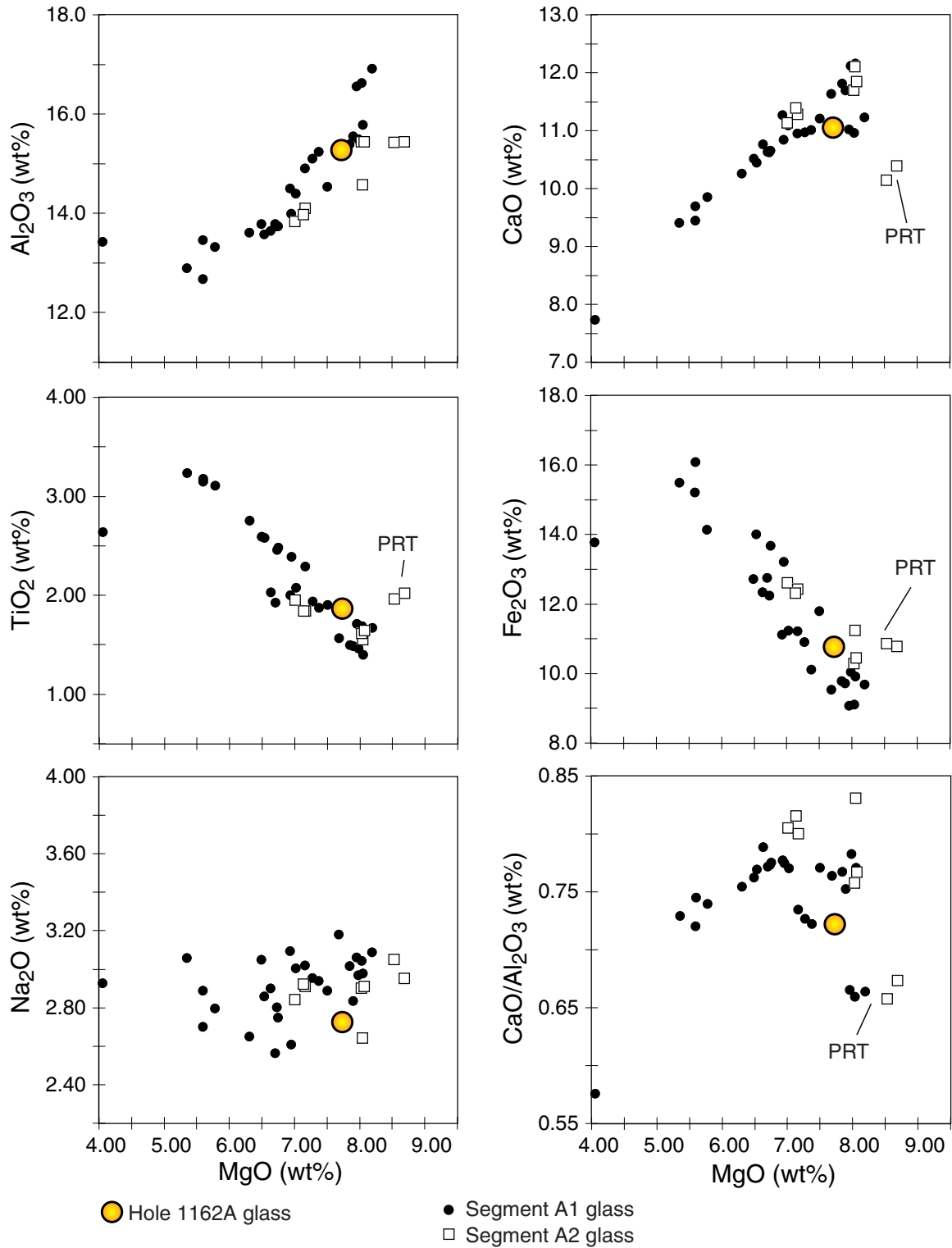
Figure F27. Trace element compositions vs. MgO for Hole 1162B basalt glass compared with Segment Al and A2 glass from Zone A. PRT = propagating rift tip lavas.
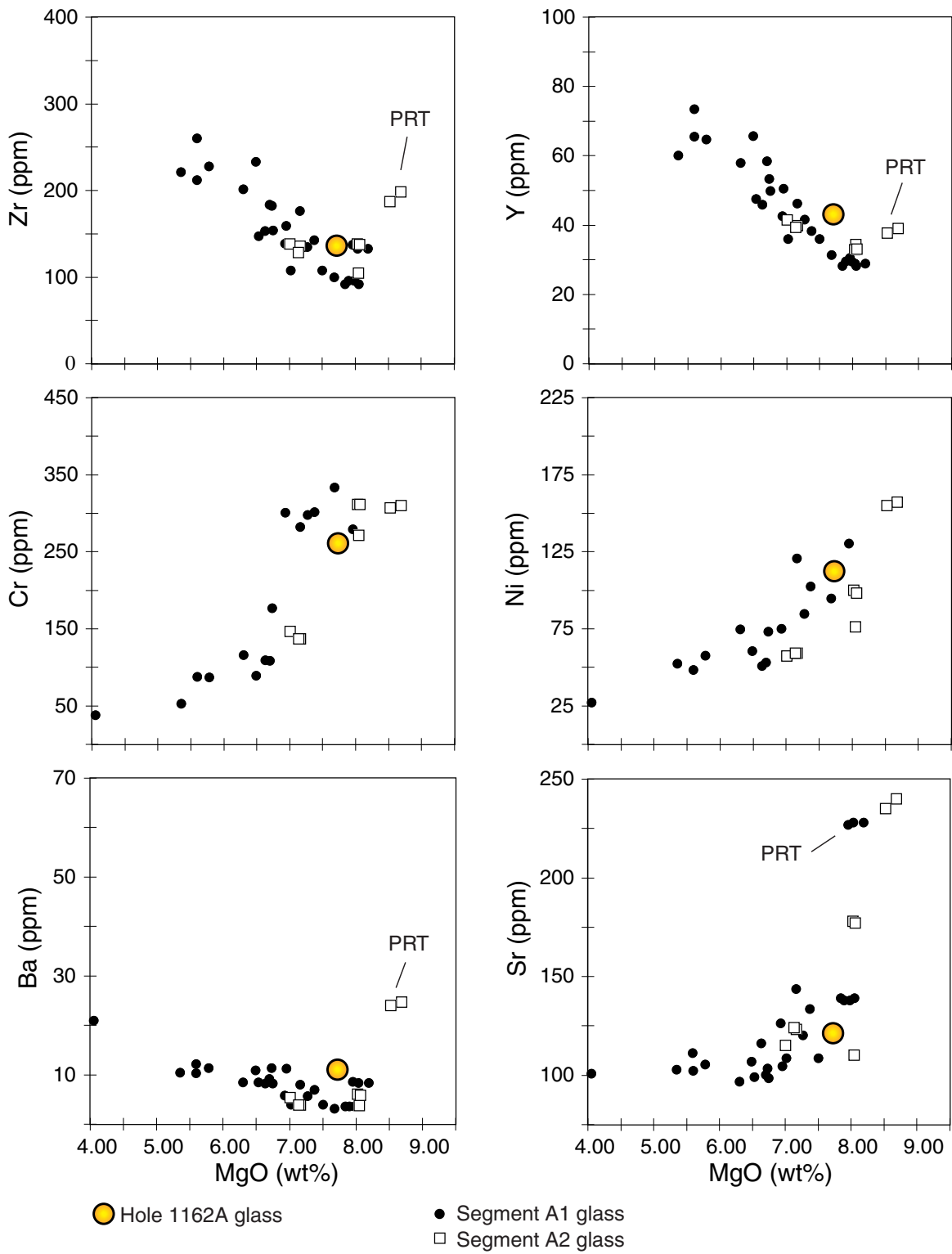
Figure F28. A. Variations of Zr/Ba vs. Ba for Hole 1162B basalt glass compared with Indian- and Pacific-type mid-ocean-ridge basalt (MORB) fields defined by zero-age Southeast Indian Ridge (SEIR) lavas dredged between 123°E and 133°E. TP = Transitional Pacific; PRT = propagating rift tip lavas. **B.** Variations of Na_2O/TiO_2 vs. MgO for Hole 1162B basalt glass compared with Segment Al and A2 glass from Zone A. The dashed line separates Indian- and Pacific-type zero-age SEIR basalt glass.
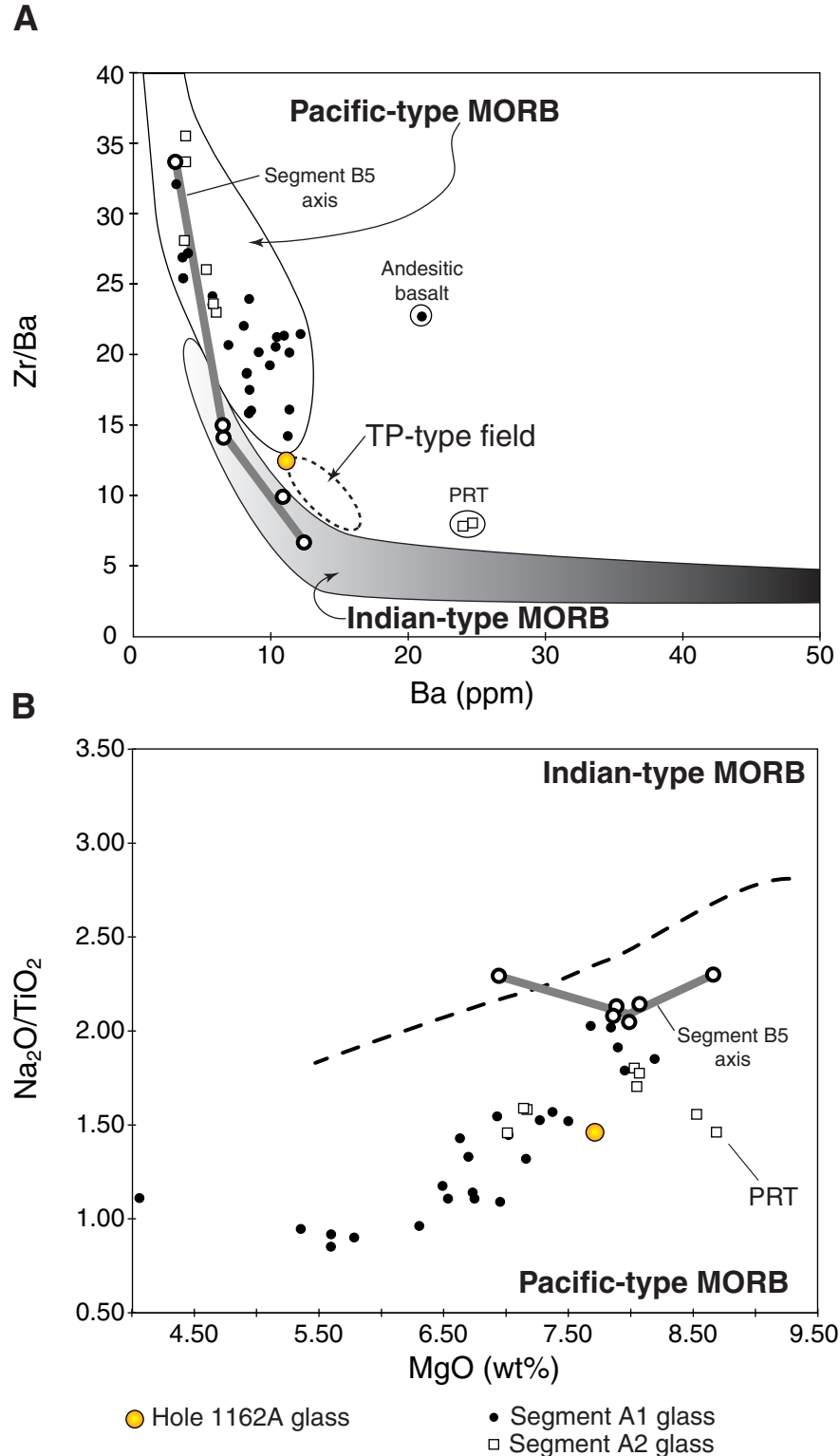
Table T1. Coring summary, Site 1162.

Hole 1162A
Latitude: 44°38.0311′S
Longitude: 129°11.2906′E
Time on hole: 1530 hr, 27 Dec 99–0100 hr, 29 Dec 99 (33.5 hr)
Time on site: 0100 hr, 29 Dec 99–1400 hr, 31 Dec 99 (94.5 hr)
Seafloor (drill-pipe measurement from rig floor, mbrf): 5475.4
Distance between rig floor and sea level (m): 11.4
Water depth (drill-pipe measurement from sea level, m): 5464.0
Total depth (from rig floor, mbrf): 5840.0
Total penetration (mbsf): 364.6
Total length of cored section (m): 31.4
Total length of drilled intervals (m): 333.2
Total core recovered (m): 2.58
Core recovery (%): 8.2
Total number of cores: 4
Total number of drilled cores: 1

Hole 1162B
Latitude: 44°37.9242′S
Longitude: 129°11.2809′E
Time on hole: 0100 hr, 29 Dec 99–1400 hr, 31 Dec 99 (61.0 hr)
Seafloor (drill-pipe measurement from rig floor, mbrf): 5475.4
Distance between rig floor and sea level (m): 11.4
Water depth (drill-pipe measurement from sea level, m): 5464.0
Total depth (from rig floor, mbrf): 5882.7
Total penetration (mbsf): 407.3
Total length of cored section (m): 58.9
Total length of drilled intervals (m): 348.4
Total core recovered (m): 9.94
Core recovery (%): 16.9
Total number of cores: 10
Total number of drilled cores: 1

Core	Date (Dec 1999)	Ship local time	Depth (mbsf) Top	Bottom	Length (m) Cored	Recovered	Recovery (%)	Comment
187-1162A-								
1W	28	1145	0.0	333.2	333.2	2.64	N/A	
2R	28	1430	333.2	340.2	7.0	0.12	1.7	Whirl-Pak
3R	28	1720	340.2	345.8	5.6	0.25	4.5	
4R	28	2005	345.8	355.2	9.4	0.70	7.4	
5R	28	2345	355.2	364.6	9.4	1.51	16.1	
			Cored:		31.4	2.58	8.2	
			Drilled:		333.2			
			Total:		364.5			
187-1162B-								
1W	29	1025	0.0	348.4	348.4	3.81	N/A	
2R	29	1320	348.4	355.0	6.6	0.91	13.8	Whirl-Pak
3R	29	1620	355.0	359.4	4.4	2.50	56.8	
4R	29	1935	359.4	364.8	5.4	1.72	31.9	
5R	29	2310	364.8	369.2	4.4	0.89	20.2	
6R	30	0250	369.2	374.2	5.0	1.42	28.4	
7R	30	0600	374.2	378.3	4.1	0.29	7.1	
8R	30	0925	378.3	383.3	5.0	0.51	10.2	
9R	30	1415	383.3	392.6	9.3	1.02	11.0	
10R	30	2025	392.6	401.6	9.0	0.42	4.7	
11R	31	0115	401.6	407.3	5.7	0.26	4.6	Whirl-Pak
			Cored:		58.9	9.94	16.9	
			Drilled:		348.4			
			Total:		407.3			

Notes: N/A = not applicable. This table is also available in **ASCII** format.

Table T2. Rock samples incubated for enrichment cultures and prepared for DNA analysis and electron microscope studies and microspheres evaluated for contamination studies.

Core	Depth (mbsf)	Sample type	Enrichment cultures			DNA analysis			SEM/TEM samples		Microspheres*	
			Anaerobic	Aerobic	High pressure	Wash	Centrifuged	Fixed	Fixed	Air dried	Exterior	Interior
187-1162A-												
2R	333.2-340.2										Yes	Yes
3R	340.2-345.8	Dolomite-cemented basalt breccia	9	3	X	X		X	X	X	Yes	X†
5R	355.2-364.6	Dolomite-cemented basalt breccia	9	3		X		X		X		
187-1162B-												
2R	348.4-355.0	Dolomite-cemented basalt breccia	7	3		X		X		X	Yes	Yes
6R	369.2-374.2	Dolomite-cemented basalt breccia	7	3		X		X				
11R	401.6-407.3										Yes	Yes
		Seawater					X	X				

Notes: SEM = scanning electron microscope; TEM = transmission electron microscopy; * = contamination test; X = samples prepared on board; † = no thin sections were made to examine the interior of the rocks for microspheres. This table is also available in **ASCII** format.

Table T3. Glass and whole-rock major and trace element compositions of basalts, Hole 1162B.

			Hole 1162B			
Core, section:	5R-1	5R-1	8R-1	8R-1	8R-1	8R-1
Interval (cm):	10-13	113-116	80-82	80-82	80-82	80-82
Depth (mbsf):	364.9	365.93	379.1	379.1	379.1	379.1
Piece:	3	24	24	24	24	24
Analysis:	ICP	ICP	ICP	ICP	ICP	ICP
Rock type:	Carbonate	Carbonate	Glass	Glass	Glass	Glass
Major element (wt%)						
SiO_2			50.30	50.33	52.07	51.65
TiO_2			1.89	1.85	1.88	1.85
Al_2O_3			15.16	15.34	15.41	15.29
Fe_2O_3			10.70	10.88	10.70	10.81
MnO			0.17	0.16	0.17	0.18
MgO	19.64	17.17	7.71	7.71	7.59	7.87
CaO	31.18	28.53	11.05	11.04	10.99	11.05
Na_2O			2.71	2.77	2.73	2.71
K_2O			0.08	0.08	0.09	0.09
P_2O_5			0.15	0.19	0.17	0.19
LOI						
CO_2						
H_2O						
Total:			99.94	100.35	101.81	101.70
Trace element (ppm)						
Nb						
Zr			134	137	145	132
Y			41	43	43	45
Sr	143	120	114	114	113	114
Rb						
Zn						
Cu						
Ni			101	99	100	103
Cr			283	287	288	301
V						
Ce						
Ba	6	3	11	11	11	12
Sc			34	37	38	36

Notes: LOI = loss on ignition. No Hole 1162A samples were analyzed. This table is also available in **ASCII** format.